

# Semi-Bayesian active learning quadrature for estimating extremely low failure probabilities

Chao Dang<sup>a,\*</sup>, Michael Beer<sup>a,b,c</sup>

<sup>a</sup>*Institute for Risk and Reliability, Leibniz University Hannover, Callinstr. 34, Hannover 30167, Germany*

<sup>b</sup>*Institute for Risk and Uncertainty, University of Liverpool, Liverpool L69 7ZF, United Kingdom*

<sup>c</sup>*International Joint Research Center for Resilient Infrastructure & International Joint Research Center for Engineering Reliability and Stochastic Mechanics, Tongji University, Shanghai 200092, PR China*

---

## Abstract

The Bayesian failure probability inference (BFPI) framework provides a sound basis for developing new Bayesian active learning reliability analysis methods. However, it is still computationally challenging to make use of the posterior variance of the failure probability. This study presents a novel method called ‘semi-Bayesian active learning quadrature’ (SBALQ) for estimating extremely low failure probabilities, which builds upon the BFPI framework. The key idea lies in only leveraging the posterior mean of the failure probability to design two crucial components for active learning - the stopping criterion and learning function. In this context, a new stopping criterion is introduced through exploring the structure of the posterior mean. Besides, we also develop a numerical integration technique named ‘hyper-shell simulation’ to estimate the analytically intractable integrals inherent in the stopping criterion. Furthermore, a new learning function is derived from the stopping criterion and by maximizing it a single point can be identified in each iteration of the active learning phase. To enable multi-point selection and facilitate parallel computing, the proposed learning function is modified by incorporating an influence function. Through five numerical examples, it is demonstrated that the proposed method can assess extremely small failure probabilities with desired efficiency and accuracy.

*Keywords:* Structural reliability analysis; Bayesian active learning; Stopping criterion; Learning function; Parallel computing

---

\*Corresponding author

Email address: [chao.dang@irz.uni-hannover.de](mailto:chao.dang@irz.uni-hannover.de) (Chao Dang)

## 1. Introduction

In the context of probabilistic structural reliability analysis, a primary objective is to compute the so-called failure probability, which is defined through a multidimensional integral as follows:

$$P_f = \int_{\mathcal{X}} I(g(\mathbf{x}) \leq 0) f_{\mathbf{X}}(\mathbf{x}) d\mathbf{x}, \quad (1)$$

where  $\mathbf{X} = [X_1, X_2, \dots, X_d] \in \mathcal{X} \subseteq \mathbb{R}^d$  is a vector of  $d$  basic random variables;  $f_{\mathbf{X}}(\mathbf{x})$  denotes the joint probability density function (PDF) of  $\mathbf{X}$ ;  $g(\cdot)$  is the performance function (also known as the limit state function), which takes a non-positive value when a prescribed failure event occurs;  $I(\cdot)$  is the indicator function:  $I = 1$  if  $g(\mathbf{x}) \leq 0$  and  $I = 0$  otherwise. An analytical solution of Eq. (1) is always desirable, which, however, is rarely available in the majority of real-world scenarios. Therefore, the use of numerical approximation becomes essential to derive a failure probability estimate. A typical numerical solution scheme involves repeatedly eventuating the  $I$ -function (equivalently, the  $g$ -function) many times. However, it is worth noting that each evaluation of the  $g$ -function may take a long running time, which poses a significant computational challenge in probabilistic structural reliability analysis.

There exist many numerical methods for approximating the failure probability, such as crude Monte Carlo simulation (MCS) [1] and its variants (e.g., important sampling [2–4], subset simulation [5], directional simulation [6] and line sampling [7]), first- and second- order reliability methods [8–10] and surrogate-based methods (e.g., polynomial chaos expansions [11] and Kriging [12]), to name just a few. The reader is referred to [13] for a relatively comprehensive review of existing computational methods for probabilistic structural reliability analysis. Among the diverse paradigms, the active learning reliability approaches have attracted increasing attention in the last decade. In this context, two seminal works are the efficient global reliability analysis [14] and the active learning reliability method combining Kriging and MCS (AK-MCS) [15]. Since their inception, a large number of active learning reliability methods have been developed. To learn about those advancements, we direct the reader to [16–18]. It has been shown that active learning reliability analysis methods can yield accurate failure probability estimates with fewer  $g$ -function calls. This is advantageous, especially for computationally demanding problems.

49 In addition, another more recent category, collectively denoted as Bayesian active learning reliability  
50 analysis methods (e.g., [19–26]), has emerged in recent years. These methods feature a distinctive fusion of  
51 Bayesian statistical inference and active learning techniques, referred to simply as Bayesian active learning.  
52 A first attempt is the ‘active learning probabilistic integration’ (ALPI) method reported in [19]. This  
53 method frames the estimation of the failure probability integral as a Bayesian inference problem, and a  
54 learning function and stopping criterion are developed based on the posterior mean and an upper bound on  
55 the posterior variance of the failure probability. The ALPI method is further enhanced to assess small failure  
56 probabilities and use parallel computing, resulting in the ‘parallel adaptive Bayesian quadrature’ (PABQ)  
57 method [20]. In the work presented in [21], the authors introduce a principled Bayesian framework known  
58 as ‘Bayesian Failure Probability Inference’ (BFPI). A noteworthy contribution is that the posterior variance  
59 of the failure probability is derived. However, it cannot be expressed in a closed form and is expensive to  
60 evaluate numerically, making it challenging to use for active learning purposes. Consequently, efforts have  
61 been made to develop Bayesian active learning reliability analysis methods that do not rely solely on the  
62 posterior variance of the failure probability. For instance, parallel Bayesian probabilistic integration [25] and  
63 partially Bayesian active learning cubature (PBALC) [26] are such methods. Besides, the Bayesian active  
64 learning concept is also investigated in the context of line sampling for structural reliability analysis [22–  
65 24]. While considerable progress has been made, there is still significant room for improvement in making  
66 Bayesian active learning reliability analysis methods more effective tools for practical applications.

67 The objective of this paper is to develop a new Bayesian active learning reliability analysis method  
68 with the capability to assess extremely low failure probabilities and facilitate parallel computing. This  
69 method relies solely on the posterior mean of the failure probability, aligning with the idea introduced in the  
70 previous work [26]. The resulting method is termed ‘semi-Bayesian active learning quadrature’ (SBALQ).  
71 The primary contributions of this work can be summarized as follows. First, a novel stopping criterion is  
72 introduced based on exploring the structure of the posterior mean of the failure probability. Second, an  
73 effective numerical integration method called ‘hyper-shell simulation’ (HSS) is developed for approximating  
74 the two intractable integrals involved in the proposed stopping criterion. Third, new learning functions are

75 designed to enable multi-point section during the active learning phase, thus facilitating parallel distributed  
 76 processing.

77 The rest of this paper is arranged as follows. In Section 2, we provide a brief review of two previous  
 78 studies. The proposed SBALQ method is introduced in Section 3. Five numerical examples are investigated  
 79 in Section 4 to illustrate the proposed method. This paper closes with some concluding remarks in Section  
 80 5.

## 81 2. Brief review of two related works

82 This section provides a brief overview of the BFPI framework [21] and the three PBALC methods [26],  
 83 which are closely related to this work. Note that both the PBALC method and the proposed SBALQ method  
 84 are set up in the standard normal space (called the  $\mathcal{U}$  space). For consistency, we will reformulate the BFPI  
 85 framework in the  $\mathcal{U}$  space. To do so, let us first introduce a transformation  $T$  (e.g., Rosenblatt transformation  
 86 and Nataf transformation) that can project the physical random vector  $\mathbf{X}$  into a standard normal one  $\mathbf{U}$ ,  
 87 i.e.,  $\mathbf{U} = T(\mathbf{X})$ , where  $\mathbf{U} = [U_1, U_2, \dots, U_d] \in \mathcal{U} \subseteq \mathbb{R}^d$  is a set of  $d$  i.i.d. standard normal variables. This  
 88 allows us to define a transformed performance function  $\mathcal{G}(\mathbf{U}) = g(T^{-1}(\mathbf{U}))$ , where  $\mathcal{G} = g \circ T^{-1}$  and  $T^{-1}$   
 89 represents the inverse transformation.

### 90 2.1. Bayesian failure probability inference

91 The BPFPI framework recast in the  $\mathcal{U}$  space begins by assigning a Gaussian process (GP) prior over the  
 92  $\mathcal{G}$ -function:

$$\mathcal{G}_0(\mathbf{u}) \sim \mathcal{GP}(m_{\mathcal{G}_0}(\mathbf{u}), k_{\mathcal{G}_0}(\mathbf{u}, \mathbf{u}')), \quad (2)$$

93 where  $\mathcal{G}_0$  represents the prior distribution of  $\mathcal{G}$  before seeing any observation data;  $m_{\mathcal{G}_0}(\mathbf{u})$  and  $k_{\mathcal{G}_0}(\mathbf{u}, \mathbf{u}')$   
 94 denote the prior mean and covariance functions, respectively, which can fully define the GP prior. Without  
 95 loss of generality, the prior mean and covariance functions are assumed to be a constant and a squared  
 96 exponential kernel, respectively:

$$m_{\mathcal{G}_0}(\mathbf{u}) = \beta, \quad (3)$$

$$k_{\mathcal{G}_0}(\mathbf{u}, \mathbf{u}') = s_0^2 \exp\left(-\frac{1}{2}(\mathbf{u} - \mathbf{u}')^\top \boldsymbol{\Sigma}^{-1}(\mathbf{u} - \mathbf{u}')\right), \quad (4)$$

98 where  $\beta \in \mathbb{R}$ ;  $s_0 > 0$  is the standard deviation of the GP prior;  $\boldsymbol{\Sigma} = \text{diag}(l_1^2, l_2^2, \dots, l_d^2)$ , where  $\text{diag}$  and  
 99  $l_i > 0$  are the diagonal operator and the length scale in the  $i$ -th dimension, respectively. The parameters  
 100 collected in  $\boldsymbol{\theta} = [\beta, s_0, l_1, l_2, \dots, l_d]$  are referred to as the hyper-parameters.

101 Now suppose that we obtain an observation dataset  $\mathcal{D} = \{\mathcal{U}, \mathcal{Y}\}$ , where  $\mathcal{U} = \{\mathbf{u}^{(j)}\}_{j=1}^n$  is an  $n \times d$   
 102 matrix with  $j$ -th row being  $\mathbf{u}^{(j)} \in \mathcal{U}$  and  $\mathcal{Y} = [y^{(1)}, y^{(2)}, \dots, y^{(n)}]^\top$  is an  $n \times 1$  vector with  $j$ -th element being  
 103  $y^{(j)} = \mathcal{G}(\mathbf{u}^{(j)})$ . Those hyper-parameters can be learned from  $\mathcal{D}$  by maximizing the log-marginal likelihood:

$$\log p(\mathcal{Y}|\mathcal{U}, \boldsymbol{\theta}) = -\frac{1}{2} [(\mathcal{Y} - \beta)^\top \mathbf{K}_{\mathcal{G}_0}^{-1}(\mathcal{Y} - \beta) + \log |\mathbf{K}_{\mathcal{G}_0}| + n \log 2\pi], \quad (5)$$

104 where  $\mathbf{K}_{\mathcal{G}_0}$  denotes an  $n \times n$  covariance matrix with its  $(i, j)$ -th entry being  $k_{\mathcal{G}_0}(\mathbf{u}^{(i)}, \mathbf{u}^{(j)})$ .

105 The posterior distribution of  $\mathcal{G}$  conditional on  $\mathcal{D}$  follows another GP:

$$\mathcal{G}_n(\mathbf{u}) \sim \mathcal{GP}(m_{\mathcal{G}_n}(\mathbf{u}), k_{\mathcal{G}_n}(\mathbf{u}, \mathbf{u}')), \quad (6)$$

106 where  $\mathcal{G}_n$  represents the posterior distribution of  $\mathcal{G}$  after seeing  $n$  observations;  $m_{\mathcal{G}_n}(\mathbf{u})$  and  $k_{\mathcal{G}_n}(\mathbf{u}, \mathbf{u}')$  are  
 107 the posterior mean and covariance functions, respectively, which can be given by:

$$m_{\mathcal{G}_n}(\mathbf{u}) = m_{\mathcal{G}_0}(\mathbf{u}) + \mathbf{k}_{\mathcal{G}_0}(\mathbf{u}, \mathcal{U})^\top \mathbf{K}_{\mathcal{G}_0}^{-1}(\mathcal{Y} - \mathbf{m}_{\mathcal{G}_0}(\mathcal{U})), \quad (7)$$

108

$$k_{\mathcal{G}_n}(\mathbf{u}, \mathbf{u}') = k_{\mathcal{G}_0}(\mathbf{u}, \mathbf{u}') - \mathbf{k}_{\mathcal{G}_0}(\mathbf{u}, \mathcal{U})^\top \mathbf{K}_{\mathcal{G}_0}^{-1} \mathbf{k}_{\mathcal{G}_0}(\mathcal{U}, \mathbf{u}'), \quad (8)$$

109 where  $\mathbf{m}_{\mathcal{G}_0}(\mathcal{U}) = [m_{\mathcal{G}_0}(\mathbf{u}^{(1)}), m_{\mathcal{G}_0}(\mathbf{u}^{(2)}), \dots, m_{\mathcal{G}_0}(\mathbf{u}^{(n)})]^\top$ ;  $\mathbf{k}_{\mathcal{G}_0}(\mathbf{u}, \mathcal{U}) = [k_{\mathcal{G}_0}(\mathbf{u}, \mathbf{u}^{(1)}), k_{\mathcal{G}_0}(\mathbf{u}, \mathbf{u}^{(2)}), \dots, k_{\mathcal{G}_0}(\mathbf{u}, \mathbf{u}^{(n)})]^\top$ ;

110  $\mathbf{k}_{\mathcal{G}_0}(\mathcal{U}, \mathbf{u}') = [k_{\mathcal{G}_0}(\mathbf{u}^{(1)}, \mathbf{u}'), k_{\mathcal{G}_0}(\mathbf{u}^{(2)}, \mathbf{u}'), \dots, k_{\mathcal{G}_0}(\mathbf{u}^{(n)}, \mathbf{u}')]^\top$ .

111 The posterior mean and variance of the failure probability  $\mathcal{P}_f$  are expressed as:

$$m_{\mathcal{P}_f, n} = \int_{\mathcal{U}} \Phi\left(-\frac{m_{\mathcal{G}_n}(\mathbf{u})}{\sigma_{\mathcal{G}_n}(\mathbf{u})}\right) \phi_{\mathcal{U}}(\mathbf{u}) d\mathbf{u}, \quad (9)$$

112

$$\begin{aligned} \sigma_{\mathcal{P}_f, n}^2 = & \int_{\mathcal{U}} \int_{\mathcal{U}} \Phi_2\left(\begin{bmatrix} 0 \\ 0 \end{bmatrix}; \begin{bmatrix} m_{\mathcal{G}_n}(\mathbf{u}) \\ m_{\mathcal{G}_n}(\mathbf{u}') \end{bmatrix}, \begin{bmatrix} \sigma_{\mathcal{G}_n}^2(\mathbf{u}) & k_{\mathcal{G}_n}(\mathbf{u}, \mathbf{u}') \\ k_{\mathcal{G}_n}(\mathbf{u}', \mathbf{u}) & \sigma_{\mathcal{G}_n}^2(\mathbf{u}') \end{bmatrix}\right) \phi_{\mathcal{U}}(\mathbf{u}) \phi_{\mathcal{U}}(\mathbf{u}') d\mathbf{u} d\mathbf{u}' \\ & - \left[ \int_{\mathcal{U}} \Phi\left(-\frac{m_{\mathcal{G}_n}(\mathbf{u})}{\sigma_{\mathcal{G}_n}(\mathbf{u})}\right) \phi_{\mathcal{U}}(\mathbf{u}) d\mathbf{u} \right]^2, \end{aligned} \quad (10)$$

113 where  $\Phi$  and  $\Phi_2$  denote the cumulative distribution function (CDF) of the standard normal variable and  
 114 bivariate normal CDF, respectively;  $\phi_{\mathbf{U}}(\cdot)$  is the joint PDF of  $\mathbf{U}$ ;  $\sigma_{\mathcal{G}_n}^2(\cdot)$  represents the posterior variance  
 115 function of  $\mathcal{G}$ , i.e.,  $\sigma_{\mathcal{G}_n}^2(\cdot) = k_{\mathcal{G}_n}(\cdot, \cdot)$ .

116 The BFPI framework actually provides a probabilistic prediction for the failure probability  $\mathcal{P}_f$ , though  
 117 the exact distribution is unknown. The posterior mean  $m_{\mathcal{P}_{f,n}}$  is a natural point estimate for  $\mathcal{P}_f$ , while the  
 118 posterior variance  $\sigma_{\mathcal{P}_{f,n}}^2$  can measure our uncertainty of the estimate. Note that both  $m_{\mathcal{P}_{f,n}}$  and  $\sigma_{\mathcal{P}_{f,n}}^2$  are  
 119 analytically intractable. Compared to  $m_{\mathcal{P}_{f,n}}$ ,  $\sigma_{\mathcal{P}_{f,n}}^2$  is harder to approximate because it involves a more  
 120 complex integral.

## 121 2.2. Partially Bayesian active learning cubature

122 The three PBALC methods (denoted as PBALC1, PBALC2, and PBALC3) further embed the BFPI  
 123 framework in an active learning circle. The underlying idea is to use only the posterior mean  $m_{\mathcal{P}_{f,n}}$  to  
 124 design crucial components for Bayesian active learning (i.e., stopping criterion and learning function), thus  
 125 avoiding the need to deal with the posterior variance  $\sigma_{\mathcal{P}_{f,n}}^2$ . The resulting three sets of stopping criteria and  
 126 learning functions are summarized in Table 1. Note that the key to achieving these results is to examine  
 127 the numerator of the fractional term inherent in the posterior mean of the failure probability  $m_{\mathcal{P}_{f,n}}$ .

Table 1: Stopping criteria and learning functions developed in PBALC1, PBALC2, and PBALC3.

| Method | Stopping criterion   | Learning function   |
|--------|--|---|
| PBALC1 | $\frac{\int_{\mathcal{U}} \left[ \Phi\left(-\frac{m_{\mathcal{G}_n}(\mathbf{u})}{\sigma_{\mathcal{G}_n}(\mathbf{u})}\right) - \Phi\left(-\frac{m_{\mathcal{G}_n}(\mathbf{u})}{\sigma_{\mathcal{G}_n}(\mathbf{u})} - b\right) \right] \phi_{\mathbf{U}}(\mathbf{u}) d\mathbf{u}}{\int_{\mathcal{U}} \Phi\left(-\frac{m_{\mathcal{G}_n}(\mathbf{u})}{\sigma_{\mathcal{G}_n}(\mathbf{u})}\right) \phi_{\mathbf{U}}(\mathbf{u}) d\mathbf{u}} < \epsilon_1$     | $\text{LSC}(\mathbf{u}) = \left[ \Phi\left(-\frac{m_{\mathcal{G}_n}(\mathbf{u})}{\sigma_{\mathcal{G}_n}(\mathbf{u})}\right) - \Phi\left(-\frac{m_{\mathcal{G}_n}(\mathbf{u})}{\sigma_{\mathcal{G}_n}(\mathbf{u})} - b\right) \right] \phi_{\mathbf{U}}(\mathbf{u})$       |
| PBALC2 | $\frac{\int_{\mathcal{U}} \left[ \Phi\left(-\frac{m_{\mathcal{G}_n}(\mathbf{u})}{\sigma_{\mathcal{G}_n}(\mathbf{u})} + b\right) - \Phi\left(-\frac{m_{\mathcal{G}_n}(\mathbf{u})}{\sigma_{\mathcal{G}_n}(\mathbf{u})}\right) \right] \phi_{\mathbf{U}}(\mathbf{u}) d\mathbf{u}}{\int_{\mathcal{U}} \Phi\left(-\frac{m_{\mathcal{G}_n}(\mathbf{u})}{\sigma_{\mathcal{G}_n}(\mathbf{u})}\right) \phi_{\mathbf{U}}(\mathbf{u}) d\mathbf{u}} < \epsilon_2$     | $\text{RSC}(\mathbf{u}) = \left[ \Phi\left(-\frac{m_{\mathcal{G}_n}(\mathbf{u})}{\sigma_{\mathcal{G}_n}(\mathbf{u})} + b\right) - \Phi\left(-\frac{m_{\mathcal{G}_n}(\mathbf{u})}{\sigma_{\mathcal{G}_n}(\mathbf{u})}\right) \right] \phi_{\mathbf{U}}(\mathbf{u})$       |
| PBALC3 | $\frac{\int_{\mathcal{U}} \left[ \Phi\left(-\frac{m_{\mathcal{G}_n}(\mathbf{u})}{\sigma_{\mathcal{G}_n}(\mathbf{u})} + b\right) - \Phi\left(-\frac{m_{\mathcal{G}_n}(\mathbf{u})}{\sigma_{\mathcal{G}_n}(\mathbf{u})} - b\right) \right] \phi_{\mathbf{U}}(\mathbf{u}) d\mathbf{u}}{\int_{\mathcal{U}} \Phi\left(-\frac{m_{\mathcal{G}_n}(\mathbf{u})}{\sigma_{\mathcal{G}_n}(\mathbf{u})}\right) \phi_{\mathbf{U}}(\mathbf{u}) d\mathbf{u}} < \epsilon_3$ | $\text{LSRSC}(\mathbf{u}) = \left[ \Phi\left(-\frac{m_{\mathcal{G}_n}(\mathbf{u})}{\sigma_{\mathcal{G}_n}(\mathbf{u})} + b\right) - \Phi\left(-\frac{m_{\mathcal{G}_n}(\mathbf{u})}{\sigma_{\mathcal{G}_n}(\mathbf{u})} - b\right) \right] \phi_{\mathbf{U}}(\mathbf{u})$ |

Note that:  $b$  is a critical value that determines the desired confidence level;  $\epsilon_1$ ,  $\epsilon_2$  and  $\epsilon_3$  are three user-defined thresholds.

128 **3. Semi-Bayesian active learning quadrature**

129 In this section, we present another novel Bayesian active learning method, called SBALQ, which is  
 130 based on the BFPI framework. This method is tailored for conducting structural reliability analysis with  
 131 extremely low failure probabilities. The core idea of the proposed method aligns with that of the three  
 132 previously developed PBALC methods. Specifically, we solely use the posterior mean  $m_{\mathcal{P}_{f,n}}$  to formulate  
 133 both the stopping criterion and learning function. However, this study focuses on the denominator rather  
 134 than the numerator in the fractional term involved in the posterior mean of the failure probability. Besides,  
 135 the proposed method allows for parallel computing while the PBALC methods do not.

136 *3.1. Stopping criterion and its numerical solution*

137 The stopping criterion is of critical importance within a Bayesian active learning reliability analysis  
 138 method, as it determines when to stop. In this context, we are looking for a stopping criterion that can  
 139 judge whether the posterior mean  $m_{\mathcal{P}_{f,n}}$ , which serves as a failure probability estimate, reaches a desired  
 140 level of accuracy. However, it is difficult to establish such a stopping criterion based on the posterior mean  
 141  $m_{\mathcal{P}_{f,n}}$  without invoking the posterior variance  $\sigma_{\mathcal{P}_{f,n}}^2$ . To overcome this dilemma, a possible means is to  
 142 explore the structure of  $m_{\mathcal{P}_{f,n}}$ .

143 As seen from Eq. (9), the integrand of  $m_{\mathcal{P}_{f,n}}$  contains the ratio of the posterior mean function  $m_{\mathcal{G}_n}(\mathbf{u})$  to  
 144 the posterior standard deviation function  $\sigma_{\mathcal{G}_n}(\mathbf{u})$ . Building upon this insight, we introduce a novel quantity  
 145 by imposing a penalty on  $\sigma_{\mathcal{G}_n}(\mathbf{u})$ . This quantity, denoted as  $Q_n(p)$ , is defined as follows:

$$Q_n(p) = \int_{\mathcal{U}} \Phi \left( -\frac{m_{\mathcal{G}_n}(\mathbf{u})}{p\sigma_{\mathcal{G}_n}(\mathbf{u})} \right) \phi_{\mathcal{U}}(\mathbf{u}) d\mathbf{u}, \quad (11)$$

146 where  $0 < p < 1$  acts as a penalty factor. Consequently, we can define the absolute difference of  $m_{\mathcal{P}_{f,n}}$  and  
 147  $Q_n(p)$ , denoted as  $\Delta_n(p)$ :

$$\begin{aligned} \Delta_n(p) &= |m_{\mathcal{P}_{f,n}} - Q_n(p)| \\ &= \left| \int_{\mathcal{U}} \Phi \left( -\frac{m_{\mathcal{G}_n}(\mathbf{u})}{\sigma_{\mathcal{G}_n}(\mathbf{u})} \right) \phi_{\mathcal{U}}(\mathbf{u}) d\mathbf{u} - \int_{\mathcal{U}} \Phi \left( -\frac{m_{\mathcal{G}_n}(\mathbf{u})}{p\sigma_{\mathcal{G}_n}(\mathbf{u})} \right) \phi_{\mathcal{U}}(\mathbf{u}) d\mathbf{u} \right| \\ &= \left| \int_{\mathcal{U}} \left[ \Phi \left( -\frac{m_{\mathcal{G}_n}(\mathbf{u})}{\sigma_{\mathcal{G}_n}(\mathbf{u})} \right) - \Phi \left( -\frac{m_{\mathcal{G}_n}(\mathbf{u})}{p\sigma_{\mathcal{G}_n}(\mathbf{u})} \right) \right] \phi_{\mathcal{U}}(\mathbf{u}) d\mathbf{u} \right|. \end{aligned} \quad (12)$$

148 Further, we can establish an upper bound for  $\Delta_n(p)$ , denoted as  $\bar{\Delta}_n(p)$ :

$$\bar{\Delta}_n(p) = \int_{\mathcal{U}} \left| \Phi \left( -\frac{m_{\mathcal{G}_n(\mathbf{u})}}{\sigma_{\mathcal{G}_n(\mathbf{u})}} \right) - \Phi \left( -\frac{m_{\mathcal{G}_n(\mathbf{u})}}{p\sigma_{\mathcal{G}_n(\mathbf{u})}} \right) \right| \phi_{\mathcal{U}}(\mathbf{u}) d\mathbf{u}. \quad (13)$$

149 To proceed, we examine the limit of  $\bar{\Delta}_n(p)$ :

$$\begin{aligned} \mathcal{L}_n &= \lim_{p \rightarrow 0} \bar{\Delta}_n(p) \\ &= \lim_{p \rightarrow 0} \int_{\mathcal{U}} \left| \Phi \left( -\frac{m_{\mathcal{G}_n(\mathbf{u})}}{\sigma_{\mathcal{G}_n(\mathbf{u})}} \right) - \Phi \left( -\frac{m_{\mathcal{G}_n(\mathbf{u})}}{p\sigma_{\mathcal{G}_n(\mathbf{u})}} \right) \right| \phi_{\mathcal{U}}(\mathbf{u}) d\mathbf{u} \\ &= \int_{\mathcal{U}} \left| \Phi \left( -\frac{m_{\mathcal{G}_n(\mathbf{u})}}{\sigma_{\mathcal{G}_n(\mathbf{u})}} \right) - I(m_{\mathcal{G}_n(\mathbf{u})}) \right| \phi_{\mathcal{U}}(\mathbf{u}) d\mathbf{u} \\ &= \int_{\mathcal{U}} \Phi \left( -\frac{|m_{\mathcal{G}_n(\mathbf{u})|}{\sigma_{\mathcal{G}_n(\mathbf{u})}} \right) \phi_{\mathcal{U}}(\mathbf{u}) d\mathbf{u}, \end{aligned} \quad (14)$$

150 where  $I$  is a indicator function:  $I(m_{\mathcal{G}_n(\mathbf{u})}) = 1$  if  $m_{\mathcal{G}_n(\mathbf{u})} < 0$  and  $I(m_{\mathcal{G}_n(\mathbf{u})}) = 0$  otherwise. Note that it  
151 is easy to show that as  $\sigma_{\mathcal{G}_n(\mathbf{u})} \rightarrow 0^+$  and  $m_{\mathcal{G}_n(\mathbf{u})} \rightarrow \mathcal{G}(\mathbf{u})$ , there exist  $\mathcal{L}_n \rightarrow 0^+$  and  $m_{\mathcal{P}_{f,n}} \rightarrow \mathcal{P}_f$ .

152 Based on these findings, we can formulate the stopping criterion as:

$$\frac{\mathcal{L}_n}{m_{\mathcal{P}_{f,n}}} < \epsilon, \quad (15)$$

153 where  $\epsilon$  is a user-defined threshold, which should be a very small positive real number. This stopping  
154 criterion implies that the proposed method stops when the value of  $\mathcal{L}_n$  becomes significantly smaller relative  
155 to  $m_{\mathcal{P}_{f,n}}$ . The choice of the stopping criterion is rather natural, since it actually constrains the upper bound  
156 of the relative error between  $m_{\mathcal{P}_{f,n}}$  and  $\lim_{p \rightarrow 0} Q_n(p)$ . In the context of active learning reliability methods,  
157 similar stopping criteria have been reported in [27, 28]. The use of the proposed stopping criterion, however,  
158 is not straightforward because it involves two analytically intractable integrals.

159 In this study, we present a novel numerical integration method, called ‘hyper-shell simulation’ (HSS),  
160 to numerically approximate both  $m_{\mathcal{P}_{f,n}}$  and  $\mathcal{L}_n$ . Our method draws inspiration from and builds upon  
161 some established methods, especially incorporating some key principles derived from the ‘importance ball  
162 sampling’ (IBS) method [20] and ‘spherical decomposition - Monte Carlo simulation’ (SD-MCS) method  
163 [29].

164 The HSS method begins by partitioning the standard normal space  $\mathcal{U}$  into  $h$  concentric hyper-spherical



165 shells, following the SD-MCS method [29]:

$$\bigcup_{i=1}^h \mathcal{U}_i = \mathcal{U}, \quad (16)$$

$$\mathcal{U}_i \cap \mathcal{U}_j = \emptyset, i \neq j, \quad (17)$$

167 where  $\mathcal{U}_i = \{\mathbf{u} | R_{i-1} \leq \|\mathbf{u}\| < R_i\}$  denotes the  $i$ -th hyper-shell,  $i = 1, 2, \dots, h$ ;  $R_{i-1}$  and  $R_i$  are the inner and  
 168 outer radius of  $\mathcal{U}_i$ , respectively. The radii,  $\{R_j\}_{j=0}^h$ , forms an ascending sequence, i.e.,  $R_0 < R_1 < \dots < R_h$ .  
 169 Apart from  $R_0 = 0$  and  $R_h = +\infty$ , one has to choose  $R_i$  ( $i = 1, 2, \dots, m - 1$ ) properly, which can be  
 170 specified as  $R_i = \sqrt{\chi_d^{-2}(1 - 10^{-i})}$ , where  $\chi_d^{-2}(\cdot)$  denotes the inverse CDF of the chi-squared distribution  
 171 with  $d$  degrees of freedom. A schematic representation of the space decomposition in two dimensions can  
 172 be found in Fig. 1(a).

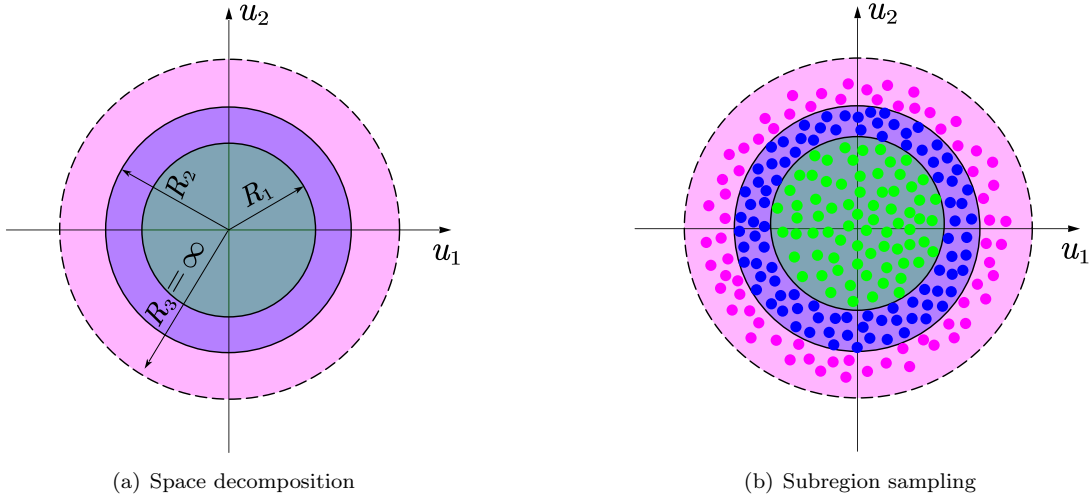


Figure 1: Illustration of the HSS method ( $h = 3$ ) in two dimensions.

173 Building upon the space decomposition, we can rewrite  $m_{\mathcal{P}_{f,n}}$  and  $\mathcal{L}_n$  as follows:

$$\begin{aligned} m_{\mathcal{P}_{f,n}} &= \sum_{i=1}^h m_{\mathcal{P}_{f,n}}^{(i)} \\ &= \sum_{i=1}^h \int_{\mathcal{U}_i} \Phi\left(-\frac{m_{\mathcal{G}_n}(\mathbf{u})}{\sigma_{\mathcal{G}_n}(\mathbf{u})}\right) \phi_{\mathcal{U}}(\mathbf{u}) d\mathbf{u}, \end{aligned} \quad (18)$$

$$\begin{aligned} \mathcal{L}_n &= \sum_{i=1}^h \mathcal{L}_n^{(i)} \\ &= \sum_{i=1}^h \int_{\mathcal{U}_i} \Phi\left(-\frac{|m_{\mathcal{G}_n}(\mathbf{u})|}{\sigma_{\mathcal{G}_n}(\mathbf{u})}\right) \phi_{\mathcal{U}}(\mathbf{u}) d\mathbf{u}. \end{aligned} \quad (19)$$

175 Then, we introduce uniform sampling PDFs (denoted as  $p^{(i)}(\mathbf{u}), i = 1, 2, \dots, h-1$ ) for the first  $h-1$   
 176 sub-regions and a truncated normal sampling PDF (denoted as  $\psi^{(h)}(\mathbf{u})$ ) for the last sub-region such that:

$$p^{(i)}(\mathbf{u}) = \begin{cases} \frac{1}{v_i}, \mathbf{u} \in \mathcal{U}_i \\ 0, \text{otherwise} \end{cases}, \quad (20)$$

$$\psi^{(h)}(\mathbf{u}) = \begin{cases} \frac{\phi_{\mathcal{U}}(\mathbf{u})}{\delta_h}, \mathbf{u} \in \mathcal{U}_h \\ 0, \text{otherwise} \end{cases}, \quad (21)$$

178 where  $v_i = \frac{\pi^{d/2}}{\Gamma(d/2+1)} (R_i^d - R_{i-1}^d)$  is the volume of the  $i$ -th hyper-shell;  $\delta_h = \int_{\mathcal{U}_h} \phi_{\mathcal{U}}(\mathbf{u}) d\mathbf{u}$  is the probability  
 179 content of the outermost hyper-shell  $\mathcal{U}_h$ . Accordingly,  $m_{\mathcal{P}_{f,n}}$  and  $\mathcal{L}_n$  can be further reformulated as:

$$\begin{aligned} m_{\mathcal{P}_{f,n}} &= \sum_{i=1}^h m_{\mathcal{P}_{f,n}}^{(i)} \\ &= \sum_{i=1}^{h-1} v_i \int_{\mathcal{U}_i} \Phi\left(-\frac{m_{\mathcal{G}_n}(\mathbf{u})}{\sigma_{\mathcal{G}_n}(\mathbf{u})}\right) \phi_{\mathcal{U}}(\mathbf{u}) p^{(i)}(\mathbf{u}) d\mathbf{u} + \delta_h \int_{\mathcal{U}_h} \Phi\left(-\frac{m_{\mathcal{G}_n}(\mathbf{u})}{\sigma_{\mathcal{G}_n}(\mathbf{u})}\right) \psi^{(h)}(\mathbf{u}) d\mathbf{u}, \end{aligned} \quad (22)$$

$$\begin{aligned} \mathcal{L}_n &= \sum_{i=1}^h \mathcal{L}_n^{(i)} \\ &= \sum_{i=1}^{h-1} v_i \int_{\mathcal{U}_i} \Phi\left(-\frac{|m_{\mathcal{G}_n}(\mathbf{u})|}{\sigma_{\mathcal{G}_n}(\mathbf{u})}\right) \phi_{\mathcal{U}}(\mathbf{u}) p^{(i)}(\mathbf{u}) d\mathbf{u} + \delta_h \int_{\mathcal{U}_h} \Phi\left(-\frac{|m_{\mathcal{G}_n}(\mathbf{u})|}{\sigma_{\mathcal{G}_n}(\mathbf{u})}\right) \psi^{(h)}(\mathbf{u}) d\mathbf{u}. \end{aligned} \quad (23)$$

181 The HSS estimators for  $m_{\mathcal{P}_{f,n}}$  and  $\mathcal{L}_n$  can be given by:

$$\begin{aligned} \hat{m}_{\mathcal{P}_{f,n}} &= \sum_{i=1}^h \hat{m}_{\mathcal{P}_{f,n}}^{(i)} \\ &= \sum_{i=1}^{h-1} v_i \left( \frac{1}{N_i} \sum_{j=1}^{N_i} \Phi\left(-\frac{m_{\mathcal{G}_n}(\mathbf{u}^{(i,j)})}{\sigma_{\mathcal{G}_n}(\mathbf{u}^{(i,j)})}\right) \phi_{\mathcal{U}}(\mathbf{u}^{(i,j)}) \right) + \delta_h \frac{1}{N_h} \sum_{j=1}^{N_h} \Phi\left(-\frac{m_{\mathcal{G}_n}(\mathbf{u}^{(h,j)})}{\sigma_{\mathcal{G}_n}(\mathbf{u}^{(h,j)})}\right), \end{aligned} \quad (24)$$

$$\begin{aligned} \hat{\mathcal{L}}_n &= \sum_{i=1}^h \hat{\mathcal{L}}_n^{(i)} \\ &= \sum_{i=1}^{h-1} v_i \left( \frac{1}{N_i} \sum_{j=1}^{N_i} \Phi\left(-\frac{|m_{\mathcal{G}_n}(\mathbf{u}^{(i,j)})|}{\sigma_{\mathcal{G}_n}(\mathbf{u}^{(i,j)})}\right) \phi_{\mathcal{U}}(\mathbf{u}^{(i,j)}) \right) + \delta_h \frac{1}{N_h} \sum_{j=1}^{N_h} \Phi\left(-\frac{|m_{\mathcal{G}_n}(\mathbf{u}^{(h,j)})|}{\sigma_{\mathcal{G}_n}(\mathbf{u}^{(h,j)})}\right), \end{aligned} \quad (25)$$

183 where  $\{\mathbf{u}^{(i,j)}\}_{j=1}^{N_i}, i = 1, 2, \dots, h-1$  is a set of  $N_i$  random samples generated according to  $p^{(i)}(\mathbf{u})$ ;  
 184  $\{\mathbf{u}^{(h,j)}\}_{j=1}^{N_h}$  is a set of  $N_h$  random samples drawn from  $\psi^{(h)}(\mathbf{u})$ . For how to generate these random numbers,  
 185 please refer to [Appendix A](#) and [Appendix B](#). In addition, one can examine Fig. [1\(b\)](#) for a visual depiction  
 186 of the sub-region sampling results.

187 The variances of the estimators can be expressed as:

$$\begin{aligned}
\text{Var} [\hat{m}_{\mathcal{P}_{f,n}}] &= \sum_{i=1}^h \text{Var} [\hat{m}_{\mathcal{P}_{f,n}}^{(i)}] \\
&= \sum_{i=1}^{h-1} \frac{1}{(N_i - 1) N_i} \sum_{j=1}^{N_i} \left[ v_i \Phi \left( -\frac{m_{\mathcal{G}_n}(\mathbf{u}^{(i,j)})}{\sigma_{\mathcal{G}_n}(\mathbf{u}^{(i,j)})} \right) \phi_{\mathcal{U}}(\mathbf{u}^{(i,j)}) - \hat{m}_{\mathcal{P}_{f,n}}^{(i)} \right]^2 \\
&\quad + \frac{1}{(N_h - 1) N_h} \sum_{j=1}^{N_h} \left[ \delta_h \Phi \left( -\frac{m_{\mathcal{G}_n}(\mathbf{u}^{(h,j)})}{\sigma_{\mathcal{G}_n}(\mathbf{u}^{(h,j)})} \right) - \hat{m}_{\mathcal{P}_{f,n}}^{(h)} \right]^2,
\end{aligned} \tag{26}$$

$$\begin{aligned}
\text{Var} [\hat{\mathcal{L}}_n] &= \sum_{i=1}^h \text{Var} [\hat{\mathcal{L}}_n^{(i)}] \\
&= \sum_{i=1}^{h-1} \frac{1}{(N_i - 1) N_i} \sum_{j=1}^{N_i} \left[ v_i \Phi \left( -\frac{|m_{\mathcal{G}_n}(\mathbf{u}^{(i,j)})|}{\sigma_{\mathcal{G}_n}(\mathbf{u}^{(i,j)})} \right) \phi_{\mathcal{U}}(\mathbf{u}^{(i,j)}) - \hat{\mathcal{L}}_n^{(i)} \right]^2 \\
&\quad + \frac{1}{(N_h - 1) N_h} \sum_{j=1}^{N_h} \left[ \delta_h \Phi \left( -\frac{|m_{\mathcal{G}_n}(\mathbf{u}^{(h,j)})|}{\sigma_{\mathcal{G}_n}(\mathbf{u}^{(h,j)})} \right) - \hat{\mathcal{L}}_n^{(h)} \right]^2,
\end{aligned} \tag{27}$$

189 where  $\text{Var} [\hat{m}_{\mathcal{P}_{f,n}}^{(i)}]$  and  $\text{Var} [\hat{\mathcal{L}}_n^{(i)}]$  are called partial variances and  $\text{Var} [\hat{m}_{\mathcal{P}_{f,n}}]$  and  $\text{Var} [\hat{\mathcal{L}}_n]$  are called total  
190 variances.

191 One of the salient features of the proposed HSS method is that it allows us to generate more samples in  
192 the hyper-shell with the largest partial variance, thus reducing the total variance more effectively. This can  
193 be achieved by the following procedure:

194 **Step A1:** Generate  $\Delta N$  initial samples in each hyper-shell, based on which the partial and total means  
195 and variances are calculated.

196 **Step A2:** Check whether the coefficients of variation are small enough, i.e.,  $\sqrt{\text{Var} [\hat{m}_{\mathcal{P}_{f,n}}]} / \hat{m}_{\mathcal{P}_{f,n}} < \gamma_1$   
197 and  $\sqrt{\text{Var} [\hat{\mathcal{L}}_n]} / \hat{\mathcal{L}}_n < \gamma_2$ , where  $\gamma_1$  and  $\gamma_2$  are two user-specified thresholds.

- 198 • If  $\sqrt{\text{Var} [\hat{m}_{\mathcal{P}_{f,n}}]} / \hat{m}_{\mathcal{P}_{f,n}} < \gamma_1$  and  $\sqrt{\text{Var} [\hat{\mathcal{L}}_n]} / \hat{\mathcal{L}}_n < \gamma_2$  are satisfied, then terminate the HSS method;
- 199 • If  $\sqrt{\text{Var} [\hat{m}_{\mathcal{P}_{f,n}}]} / \hat{m}_{\mathcal{P}_{f,n}} \geq \gamma_1$  and  $\sqrt{\text{Var} [\hat{\mathcal{L}}_n]} / \hat{\mathcal{L}}_n < \gamma_2$ , then identify the hyper-shell with the largest  
200 partial variance for  $\hat{m}_{\mathcal{P}_{f,n}}$  as  $i^* = \arg \max_{1 \leq i \leq h} \text{Var} [\hat{m}_{\mathcal{P}_{f,n}}^{(i)}]$  and go to **Step A3**;
- 201 • If  $\sqrt{\text{Var} [\hat{m}_{\mathcal{P}_{f,n}}]} / \hat{m}_{\mathcal{P}_{f,n}} < \gamma_1$  and  $\sqrt{\text{Var} [\hat{\mathcal{L}}_n]} / \hat{\mathcal{L}}_n \geq \gamma_2$ , then identify the hyper-shell with the largest  
202 partial variance for  $\hat{\mathcal{L}}_n$  as  $i^* = \arg \max_{1 \leq i \leq h} \text{Var} [\hat{\mathcal{L}}_n^{(i)}]$  and go to **Step A3**;
- 203 • If  $\sqrt{\text{Var} [\hat{m}_{\mathcal{P}_{f,n}}]} / \hat{m}_{\mathcal{P}_{f,n}} \geq \gamma_1$  and  $\sqrt{\text{Var} [\hat{\mathcal{L}}_n]} / \hat{\mathcal{L}}_n \geq \gamma_2$ , then identify the two hyper-shells with the  
204 largest partial variances for  $\hat{m}_{\mathcal{P}_{f,n}}$  and  $\hat{\mathcal{L}}_n$  as  $i_1^* = \arg \max_{1 \leq i \leq h} \text{Var} [\hat{m}_{\mathcal{P}_{f,n}}^{(i)}]$  and  $i_2^* = \arg \max_{1 \leq i \leq h} \text{Var} [\hat{\mathcal{L}}_n^{(i)}]$ ,

205 and go to **Step A4**;

206 **Step A3:** Start by generating an additional set of  $\Delta N$  samples for the  $i^*$ -th hyper-shell. Afterward,  
207 update the partial and total means and variances, and proceed to **Step A2**;

208 **Step A4:** For both the  $i_1^*$ -th and  $i_2^*$ -th hyper-shells, generate an additional set of  $\Delta N$  samples for each.  
209 Subsequently, update the partial and total means and variances before proceeding to **Step A2**;

210 The numerator and denominator on the left-hand side of the stopping criterion (Eq. (15)) should thus  
211 be replaced by the corresponding final estimates  $\hat{m}_{\mathcal{P}_{f,n}}$  and  $\hat{\mathcal{L}}_n$ . To avoid false convergence, the stopping  
212 criterion needs to be satisfied twice in a row.

### 213 3.2. Learning function and multi-point selection

214 In addition to the stopping criterion, another pivotal component for developing a Bayesian active learning  
215 reliability analysis method is the so-called learning (or acquisition) function. This function guides the active  
216 learning process by selecting the most informative data points. These carefully chosen data points, once  
217 evaluated, are expected to yield the most significant improvement on the accuracy of the failure probability  
218 prediction. Assuming that the accuracy of the failure probability prediction can be effectively governed  
219 by the proposed stopping criterion (Eq. (15)), then the optimal learning function is one that minimizes  
220 the number of selected data points required to meet this criterion. Therefore, our underlying principle for  
221 designing the learning function is to align with the attainment of the stopping criterion. Besides, we also  
222 seek to develop a strategy that can identify multiple informative points instead of a single point in each  
223 iteration from the designated learning function, in order to facilitate parallel computing.

224 A new learning function, denoted as  $\mathcal{J}_n$ , which is derived from the proposed stopping criterion, is given  
225 as follows:

$$\mathcal{J}_n(\mathbf{u}) = \Phi\left(-\frac{|m_{\mathcal{G}_n}(\mathbf{u})|}{\sigma_{\mathcal{G}_n}(\mathbf{u})}\right) \phi_{\mathbf{U}}(\mathbf{u}). \quad (28)$$

226 Note that the equation  $\int_{\mathcal{U}} \mathcal{J}_n(\mathbf{u}) d\mathbf{u} = \mathcal{L}_n$  holds. Consequently, we can interpret the learning function  $\mathcal{J}_n$   
227 as a measure that quantifies the contribution of the value at point  $\mathbf{u}$  to the overall value of  $\mathcal{L}_n$ . Intuitively,  
228 the point with the largest  $\mathcal{J}_n$ -function value is likely to be the most promising candidate point to choose.

229 It is worth pointing out that some existing learning functions can be regarded as variants of our proposed  
 230  $\mathcal{J}_n$  function, e.g.,  $U$  function [15], expected misclassification probability contribution (EMPC) function [21]  
 231 and learning functions in [27, 30].

232 Having established the learning function, we now turn our attention to the selection of multiple infor-  
 233 mative points from it. The method we are going to develop is strongly inspired by the previous work [31],  
 234 where a multi-point expected improvement criterion was proposed for efficient global optimization. It is  
 235 important to note that  $\mathcal{J}_n$  is non-negative, and drops sharply to zero at those sampled points. This inherent  
 236 property presents a promising avenue for developing a multi-point selection strategy. Suppose that in a  
 237 given iteration of active learning, we wish to select an additional  $n_a$  points, in addition to the existing  $n$   
 238 points. The core of our strategy is to select the  $n_a$  points one at a time, rather than all at once. This can be  
 239 achieved by sequentially adjusting the  $\mathcal{J}_n$  function to account for the possible effects induced by the points  
 240 that have been identified. To initiate the process, we begin by identifying the first point, denoted as  $\mathbf{u}^{(n+1)}$ ,  
 241 by maximizing the original  $\mathcal{J}_n$  function:

$$\mathbf{u}^{(n+1)} = \arg \max_{\mathbf{u} \in [-B, B]^d} \mathcal{J}_n(\mathbf{u}), \quad (29)$$

242 where  $[-B, B]^d$  is a  $d$ -dimensional hyperrectangle of side length  $B$  in the standard normal space. A con-  
 243 venient way to specify a reasonable value for  $B$  is according to  $R = \sqrt{\chi_d^{-2}(1 - \varepsilon)}$ , where  $\varepsilon = 1 \times 10^{-10}$  is  
 244 adopted [26]. Then, one can choose the  $q$ -th point  $\mathbf{u}^{(n+q)}$  by maximizing a pseudo  $\mathcal{J}_{n+q}$  function (denoted  
 245 as  $\mathcal{S}\mathcal{J}_n^{(q)}$ ) such that:

$$\mathbf{u}^{(n+q)} = \arg \max_{\mathbf{u} \in [-B, B]^d} \mathcal{S}\mathcal{J}_n^{(q)}(\mathbf{u}; \mathbf{u}^{(n+1)}, \mathbf{u}^{(n+2)}, \dots, \mathbf{u}^{(n+q-1)}). \quad (30)$$

246 Here  $\mathcal{S}\mathcal{J}_n^{(q)}$  is used to approximate the real  $\mathcal{J}_{n+q}$  function without evaluating the last  $q - 1$  points on the  $\mathcal{G}$   
 247 function. The  $\mathcal{S}\mathcal{J}_n^{(q)}$  function takes the following form:

$$\mathcal{S}\mathcal{J}_n^{(q)}(\mathbf{u}; \mathbf{u}^{(n+1)}, \mathbf{u}^{(n+2)}, \dots, \mathbf{u}^{(n+q-1)}) = \mathcal{J}_n(\mathbf{u}) \times \prod_{j=1}^{q-1} IF(\mathbf{u}, \mathbf{u}^{(n+j)}), \quad (31)$$

248 where  $IF(\mathbf{u}, \mathbf{u}^{(n+j)})$  is the influence function, defined by [31]:

$$\begin{aligned}
 IF(\mathbf{u}, \mathbf{u}^{(n+j)}) &= 1 - \rho(\mathbf{u}, \mathbf{u}^{(n+j)}) \\
 &= 1 - \exp\left(-\frac{1}{2}(\mathbf{u} - \mathbf{u}^{(n+j)})\boldsymbol{\Sigma}^{-1}(\mathbf{u} - \mathbf{u}^{(n+j)})^\top\right),
 \end{aligned}
 \tag{32}$$

249 in which  $\rho(\mathbf{u}, \mathbf{u}^{(n+j)})$  denotes the correlation coefficient function. By introducing the influence function,  
 250 the  $\mathcal{S}\mathcal{J}_n^{(q)}$  function takes a zero value at the  $q - 1$  already selected points  $\mathbf{u}^{(n+1)}, \mathbf{u}^{(n+2)}, \dots, \mathbf{u}^{(n+q-1)}$ , and  
 251 approaches to the original  $\mathcal{J}_{n+q}$  function when far away from those points. This function is referred to as  
 252 ‘pseudo’ because its primary purpose is to serve as an approximation for the true  $\mathcal{J}_{n+q}$  function. To produce  
 253  $n_a$  points in a given iteration using the proposed strategy, it is necessary to perform  $n_a$  optimizations on the  
 254 corresponding learning functions. Fortunately, this computational burden is typically much smaller than  
 255 that of a single evaluation of the  $\mathcal{G}$ -function in practical scenarios.

### 256 3.3. Implementation procedure of the proposed method

257 The main steps for implementing the proposed SBALQ method are summarized below, alongside a  
 258 flowchart shown in Fig. 2.

#### 259 **Step B1: Generate an initial observation dataset**

260 To begin the proposed method, it is necessary to create an initial observation dataset by evaluating the  
 261  $\mathcal{G}$ -function. This can be achieved by first generating a small number (denoted as  $n_0$ ) of uniformly distributed  
 262 samples  $\mathcal{U} = \{\mathbf{u}^{(j)}\}_{j=1}^{n_0}$  within a  $d$ -ball of radius  $B$  using a low-discrepancy sequence. In this study, the  
 263 radius is specified as  $B = \sqrt{\chi_d^{-2}(1 - \nu)}$  with  $\nu = 10^{-8}$ , and the Hammersley sequence is employed. Next,  
 264 the corresponding output values  $\mathcal{Y} = [y^{(1)}, y^{(2)}, \dots, y^{(n_0)}]^\top$  of the  $\mathcal{G}$ -function at  $\mathcal{U}$  can be obtained through  
 265 parallel computation. Finally, the initial observation dataset is formed by  $\mathcal{D} = \{\mathcal{U}, \mathcal{Y}\}$ . Let  $n = n_0$ .

#### 266 **Step B2: Obtain the GP posterior of the $\mathcal{G}$ -function**

267 This step entails obtaining the posterior distribution of the  $\mathcal{G}$ -function (i.e.,  $\mathcal{GP}(m_{\mathcal{G}_n}(\mathbf{u}), k_{\mathcal{G}_n}(\mathbf{u}, \mathbf{u}'))$ ),  
 268 given the data  $\mathcal{D}$ . Such task can be accomplished using some well-established GP regression toolkits. In  
 269 this study, we utilize the *fitrgp* function from the Statistics and Machine Learning Toolbox in Matlab.

#### 270 **Step B3: Compute the two integrals in the stopping criterion**

271 In this stage, one needs to compute the two estimates  $\hat{m}_{\mathcal{P}_{f,n}}$  and  $\hat{\mathcal{L}}_n$  by using the proposed HSS method  
 272 outlined in Section 3.1.

273 **Step B4: Check the stopping criterion**

274 If  $\frac{\hat{\mathcal{L}}_n}{\hat{m}_{\mathcal{P}_{f,n}}} < \epsilon$  is met twice in a row, go to **Step B6**; Otherwise, go to **Step B5**.

275 **Step B5: Enrich the observation dataset**

276 In this phase, the current observation dataset needs to be enriched with new data. First, identify the next  
 277  $n_a$  point(s)  $\mathcal{U}^+ = \{\mathbf{u}^{(n+j)}\}_{j=1}^{n_a}$  by optimizing the proposed learning function(s), where the genetic algorithm  
 278 is used in this study. Then, the evaluation of the  $\mathcal{G}$ -function at  $\mathcal{U}^+$  can be performed in parallel, which yields  
 279 the output value(s)  $\mathcal{Y}^+$ . Finally, the enriched observation dataset can be formulated as  $\mathcal{D} = \mathcal{D} \cup \{\mathcal{U}^+, \mathcal{Y}^+\}$ .

280 Let  $n = n + n_a$  and proceed to **Step B2**.

281 **Step B6: End the method**

282 Return the current estimate  $\hat{m}_{\mathcal{P}_{f,n}}$  as the failure probability estimate and end the entire procedure.

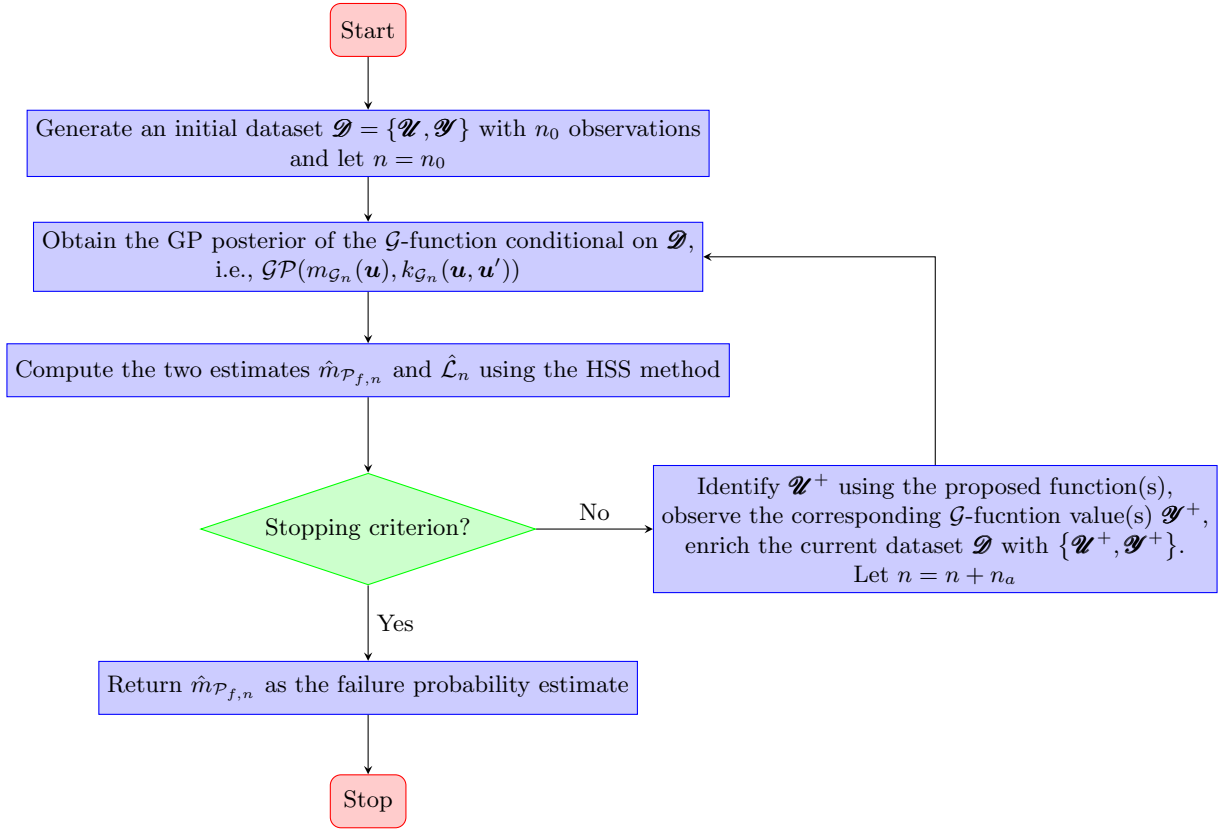


Figure 2: Flowchart of the proposed SBALQ method.

283 One must specify at least the parameters  $n_0$ ,  $h$ ,  $\Delta N$ ,  $\gamma_1$ ,  $\gamma_2$  and  $\epsilon$  before running the SBALQ algorithm.  
 284 Although they all have a clear physical meaning, some experience may be required to set the proper values.  
 285 For example, the size of the initial observed dataset  $n_0$  should be neither too small nor too large. On the  
 286 one hand, too small  $n_0$  can result in a very coarse initial GP posterior model, which is less informative for  
 287 subsequent active learning. On the other hand, too large  $n_a$  is neither necessary nor unadvisable.

#### 288 4. Numerical examples

289 Five numerical examples are analyzed in this section to demonstrate the effectiveness of the SBALQ  
 290 method in estimating extremely small failure probabilities. In each of these examples, the parameters not yet  
 291 specified in the proposed method are set to be:  $n_0 = 10$ ,  $h = 10$ ,  $\Delta N = 2 \times 10^5$ ,  $\gamma_1 = \gamma_2 = 2\%$ ,  $\epsilon = 2\%(4\%)$ .  
 292 Additionally, we vary the value of  $n_a$  to systematically investigate its influence on the obtained results. For  
 293 comparison, several representative existing methods, i.e., PBALC1 [26], PBALC2 [26], PBALC3 [26], PABQ  
 294 [20] and extreme AK-MCS (eAK-MCS) [32] are also conducted. These methods and the proposed method  
 295 are run independently 20 times to evaluate their robustness. Where it is feasible to do so, the reference  
 296 failure probabilities are generated using the MCS method with a significantly large number of simulations.

##### 297 4.1. Example 1: A series system with four branches

298 The first example involves a series system comprising four branches, which has been extensively studied  
 299 as a benchmark (see for example [15, 29, 33]). The performance function is given as follows:

$$g(X_1, X_2) = \min \begin{cases} a + \frac{(X_1 - X_2)^2}{10} - \frac{(X_1 + X_2)}{\sqrt{2}} \\ a + \frac{(X_1 - X_2)^2}{10} + \frac{(X_1 + X_2)}{\sqrt{2}} \\ (X_1 - X_2) + \frac{b}{\sqrt{2}} \\ (X_2 - X_1) + \frac{b}{\sqrt{2}} \end{cases}, \quad (33)$$

300 where  $X_1$  and  $X_2$  are two independent standard normal variables;  $a$  and  $b$  are two constant parameters,  
 301 which are specified as 6 and 12, respectively.



302 Table 2 summarizes the results of several structural reliability analysis methods. The reference failure  
 303 probability, obtained thorough the MCS method with  $10^{13}$  samples, is  $3.04 \times 10^{-9}$  with a COV of 0.57%.  
 304 When  $n_a = 1$  (indicating that parallel computing is not permitted during the active learning phase), the  
 305 proposed SBALQ method requires an average number of 32.15 iterations, which stands as the lowest among  
 306 PBACLC1, PBACLC2 and PBACLC3, while producing a fairly good average failure probability with a  
 307 small COV. When considering the case  $n_a = 4$ , the PABQ method demands more iterations on average  
 308 compared to the proposed method. The results of eAK-MCS are missing because it is unable to converge in  
 309 this example. The proposed method ( $n_a = 4$ ) can give a fairly good failure probability mean with a small  
 310 COV at the expense of only 12.75 iterations (on average). As for the proposed method itself, it can always  
 311 produce nearly unbiased results with COVs less than 4% when  $n_a$  varies from 1 to 8. Besides, it is evident  
 312 that the average number of  $\mathcal{G}$ -function calls increases with  $n_a$ , while the average number of iterations first  
 313 decreases, stays the same, and then finally increases. This observation implies that selecting an excessive  
 314 number of points at each iteration may not necessarily lead to a reduction in the overall number of iterations.

315 For a more intuitive illustration, Fig. 3 shows the selected points and convergence curve obtained from a  
 316 typical run of the proposed method ( $\epsilon = 2\%$  and  $n_a = 2$ ). As evident in Figure 3(a), a majority of the points  
 317 chosen during the active learning phase are clustered around the four critical regions of the actual limit state  
 318 curve. As we continue to identify more informative points, Figure 3(b) illustrates how the posterior failure  
 319 probability estimate gradually approaches the reference value before the stopping criterion is reached. These  
 320 observations indicate the effectiveness of the proposed learning functions and stopping criterion.

#### 321 4.2. Example 2: A nonlinear oscillator

322 As a second example, we consider a nonlinear oscillator subject to a rectangular pulse load [34], as shown  
 323 in Fig. 4. The performance function reads:

$$324 \quad g(m, k_1, k_2, r, F_1, t_1) = 3r - \left| \frac{2F_1}{k_1 + k_2} \sin \left( \frac{t_1}{2} \sqrt{\frac{k_1 + k_2}{m}} \right) \right|, \quad (34)$$

325 where  $m$ ,  $k_1$ ,  $k_2$ ,  $r$ ,  $F_1$  and  $t_1$  are six random variables, as listed in Table 3.

326 The results of several structural reliability analysis methods are reported in Table 4. The reference value

Table 2: Reliability analysis results of Example 1 by several methods.

| Method                               |           | $N_{iter}$ | $N_{call}$ | $\hat{P}_f$           | $\delta_{\hat{P}_f}$ |
|--------------------------------------|-----------|------------|------------|-----------------------|----------------------|
| MCS                                  |           | -          | $10^{13}$  | $3.04 \times 10^{-9}$ | 0.57%                |
| PBALC1 ( $\epsilon_1 = 2.5\%$ ) [26] | $n_a = 1$ | 35.75      | 44.75      | $3.04 \times 10^{-9}$ | 3.82%                |
| PBALC2 ( $\epsilon_2 = 2.5\%$ ) [26] | $n_a = 1$ | 41.10      | 50.10      | $3.04 \times 10^{-9}$ | 1.39%                |
| PBALC3 ( $\epsilon_3 = 5.0\%$ ) [26] | $n_a = 1$ | 40.50      | 49.50      | $3.03 \times 10^{-9}$ | 1.99%                |
| PABQ                                 | $n_a = 4$ | 18.00      | 78.00      | $2.95 \times 10^{-9}$ | 1.06%                |
| eAK-MCS                              | $n_a = 4$ | -          | -          | -                     | -                    |
|                                      | $n_a = 1$ | 32.15      | 41.15      | $3.03 \times 10^{-9}$ | 1.31%                |
|                                      | $n_a = 2$ | 19.35      | 46.70      | $3.03 \times 10^{-9}$ | 0.58%                |
|                                      | $n_a = 3$ | 15.55      | 53.65      | $3.01 \times 10^{-9}$ | 0.75%                |
|                                      | $n_a = 4$ | 12.75      | 57.00      | $3.02 \times 10^{-9}$ | 0.80%                |
| Proposed SBALQ ( $\epsilon = 2\%$ )  | $n_a = 5$ | 11.10      | 60.50      | $3.02 \times 10^{-9}$ | 0.68%                |
|                                      | $n_a = 6$ | 9.95       | 63.70      | $3.03 \times 10^{-9}$ | 0.48%                |
|                                      | $n_a = 7$ | 9.95       | 72.65      | $3.03 \times 10^{-9}$ | 0.44%                |
|                                      | $n_a = 8$ | 10.65      | 87.20      | $3.00 \times 10^{-9}$ | 3.98%                |

Note:  $N_{iter}$  = the total number of iterations;  $N_{call}$  = the total number of performance function calls;  $\hat{P}_f$  = the failure probability estimate;  $\delta_{\hat{P}_f}$  = the COV of  $\hat{P}_f$ .

326 of the failure probability is taken as  $4.04 \times 10^{-8}$  (with a COV of 0.50%), which is produced by the MCS  
327 method with  $10^{12}$  samples. In the non-parallel case (i.e., when  $n_a = 1$ ), the proposed SBALQ method  
328 performs similarly to PBALC1, PBALC2, and PBALC3, with a slightly smaller COV. In the parallel case  
329 (i.e., when  $n_a = 4$ ), the proposed method requires fewer iterations on average compared to the PABQ and  
330 eAK-MCS methods. However, the proposed method exhibits a smaller COV of 1.40% compared to the  
331 PABQ and eAK-MCS methods, which have COVs of 7.48% and 3.92%, respectively. In all eight cases, the

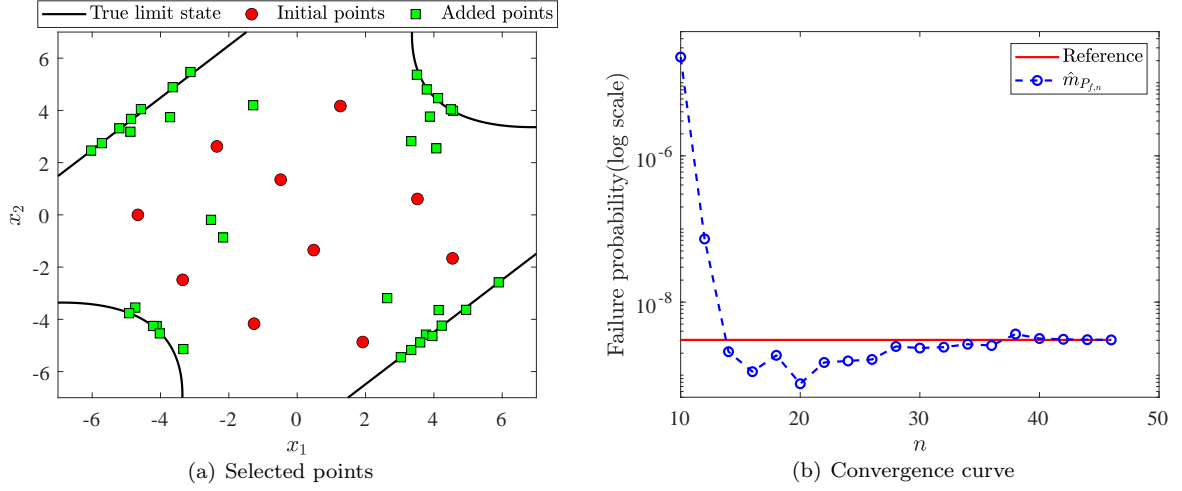


Figure 3: Illustration of the proposed SBALQ method ( $\epsilon = 2\%$  and  $n_a = 2$ ) for Example 1.

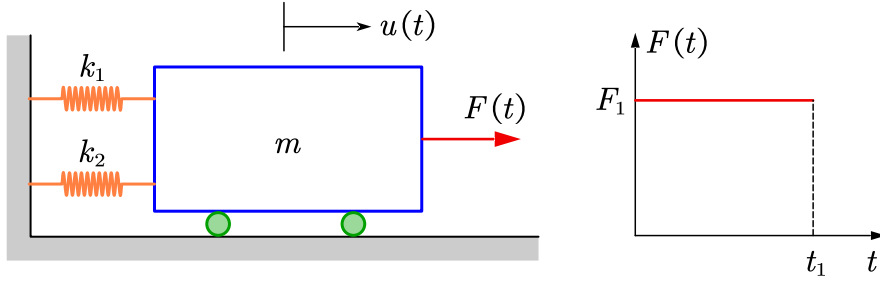


Figure 4: A nonlinear oscillator subject to a rectangular pulse load.

332 proposed method can give a nearly unbiased average failure probability with a small COV. Notably, the  
 333 average number of iterations can be reduced from 22.45 to 6.20 as  $n_a$  increases from 1 to 8.

### 334 4.3. Example 3: A reinforced concrete section

335 The third example consists of a reinforced concrete section under a bending moment [35], as depicted in  
 336 Fig. 5. The performance function can be expressed as:

$$g(\mathbf{X}) = X_1 X_2 X_3 - \frac{X_1^2 X_2^2 X_4}{X_5 X_6} - X_7, \quad (35)$$

337 where  $X_1$  to  $X_7$  are seven random variables, as shown in Table 5.

338 Table 6 lists the results of several different methods. The reference failure probability generated by the  
 339 MCS method (with  $5 \times 10^{11}$  samples) is  $1.59 \times 10^{-8}$  (with a COV of 0.79%). In the non-parallel case (i.e.,

Table 3: Random variables for Example 2.

| Variable | Description        | Distribution | Mean | COV  |
|----------|--------------------|--------------|------|------|
| $m$      | Mass               | Lognormal    | 1.0  | 0.05 |
| $k_1$    | Stiffness          | Lognormal    | 1.0  | 0.10 |
| $k_2$    | Stiffness          | Lognormal    | 0.2  | 0.10 |
| $r$      | Yield displacement | Lognormal    | 0.5  | 0.10 |
| $F_1$    | Load amplitude     | Lognormal    | 0.4  | 0.20 |
| $t_1$    | Load duration      | Lognormal    | 1.0  | 0.20 |

Table 4: Reliability analysis results of Example 2 by several methods.

| Method                              |           | $N_{iter}$ | $N_{call}$ | $\hat{P}_f$           | $\delta_{\hat{P}_f}$ |
|-------------------------------------|-----------|------------|------------|-----------------------|----------------------|
| MCS                                 | -         | -          | $10^{12}$  | $4.04 \times 10^{-8}$ | 0.50%                |
| PBALC1 ( $\epsilon_1 = 5\%$ ) [26]  | $n_a = 1$ | 20.10      | 29.10      | $4.03 \times 10^{-8}$ | 4.29%                |
| PBALC2 ( $\epsilon_2 = 5\%$ ) [26]  | $n_a = 1$ | 22.90      | 31.90      | $4.07 \times 10^{-8}$ | 2.61%                |
| PBALC3 ( $\epsilon_3 = 10\%$ ) [26] | $n_a = 1$ | 21.95      | 30.95      | $4.05 \times 10^{-8}$ | 3.66%                |
| PABQ                                | $n_a = 4$ | 9.40       | 43.60      | $3.94 \times 10^{-8}$ | 7.48%                |
| eAK-MCS                             | $n_a = 4$ | 11.35      | 51.40      | $4.05 \times 10^{-8}$ | 3.92%                |
|                                     | $n_a = 1$ | 22.45      | 31.45      | $4.03 \times 10^{-8}$ | 1.72%                |
|                                     | $n_a = 2$ | 13.35      | 34.70      | $4.09 \times 10^{-8}$ | 2.08%                |
|                                     | $n_a = 3$ | 10.00      | 37.00      | $4.03 \times 10^{-8}$ | 1.95%                |
|                                     | $n_a = 4$ | 8.50       | 40.00      | $4.05 \times 10^{-8}$ | 1.40%                |
| Proposed SBALQ ( $\epsilon = 4\%$ ) | $n_a = 5$ | 7.95       | 44.75      | $4.04 \times 10^{-8}$ | 1.12%                |
|                                     | $n_a = 6$ | 7.20       | 47.20      | $4.02 \times 10^{-8}$ | 1.95%                |
|                                     | $n_a = 7$ | 6.45       | 48.15      | $4.06 \times 10^{-8}$ | 1.74%                |
|                                     | $n_a = 8$ | 6.20       | 51.60      | $4.04 \times 10^{-8}$ | 1.48%                |

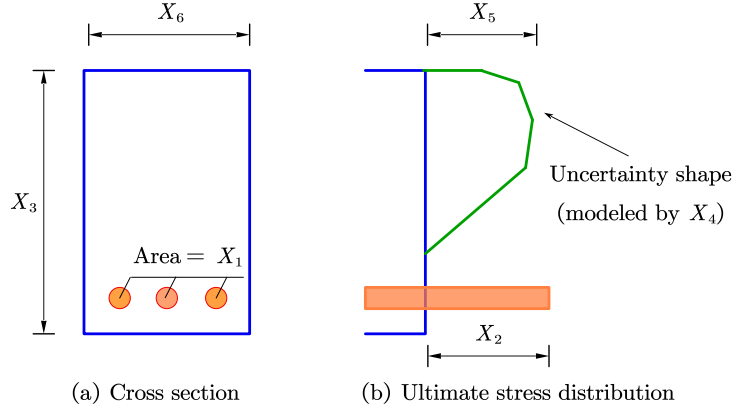


Figure 5: Ultimate stress state of a reinforced concrete section subject to a bending moment.

Table 5: Basic random variables for Example 3.

| Variable | Description                      | Distribution | Mean                  | COV  |
|----------|----------------------------------|--------------|-----------------------|------|
| $X_1$    | Area of reinforcement            | Normal       | 1260 mm <sup>2</sup>  | 0.05 |
| $X_2$    | Yield stress of reinforcement    | Lognormal    | 300 N/mm <sup>2</sup> | 0.10 |
| $X_3$    | Effective depth of reinforcement | Normal       | 770 mm                | 0.05 |
| $X_4$    | Stress-strain factor of concrete | Lognormal    | 0.35                  | 0.10 |
| $X_5$    | Compressive strength of concrete | Lognormal    | 30 N/mm <sup>2</sup>  | 0.15 |
| $X_6$    | Width of section                 | Normal       | 400 mm                | 0.05 |
| $X_7$    | Applied bending moment           | Lognormal    | 80 kN·m               | 0.20 |

<sup>340</sup>  $n_a = 1$ ), the proposed method performs slightly better than PBALC1, PBALC2 and PBALC3 . When  
<sup>341</sup>  $N_a = 4$ , the PABQ and eAK-MCS methods require fewer iterations than the proposed method. However,  
<sup>342</sup> they exhibit COVs of 12.90% and 7.17%, respectively, which are much larger than that of the proposed  
<sup>343</sup> method (1.50%). As  $n_a$  increases from 1 to 8, the proposed method can produce fairly good results with  
<sup>344</sup> almost no bias and a small COV, while significantly reducing the average number of iterations.

Table 6: Reliability analysis results of Example 3 by several methods.

| Method                              |           | $N_{iter}$ | $N_{call}$ | $\hat{P}_f$           | $\delta_{\hat{P}_f}$ |
|-------------------------------------|-----------|------------|------------|-----------------------|----------------------|
| MCS                                 |           | -          | $10^{12}$  | $1.59 \times 10^{-8}$ | 0.79%                |
| PBALC1 ( $\epsilon_1 = 5\%$ )       | $n_a = 1$ | 14.70      | 23.70      | $1.60 \times 10^{-8}$ | 3.16%                |
| PBALC2 ( $\epsilon_2 = 5\%$ )       | $n_a = 1$ | 16.45      | 25.45      | $1.57 \times 10^{-8}$ | 2.63%                |
| PBALC3 ( $\epsilon_3 = 10\%$ )      | $n_a = 1$ | 16.10      | 25.10      | $1.59 \times 10^{-8}$ | 3.37%                |
| PABQ                                | $n_a = 4$ | 6.75       | 33.00      | $1.58 \times 10^{-8}$ | 12.90%               |
| eAK-MCS                             | $n_a = 4$ | 5.40       | 27.60      | $1.60 \times 10^{-8}$ | 7.17%                |
| Proposed SBALQ ( $\epsilon = 4\%$ ) | $n_a = 1$ | 14.60      | 23.60      | $1.58 \times 10^{-8}$ | 2.35%                |
|                                     | $n_a = 2$ | 9.95       | 27.90      | $1.58 \times 10^{-8}$ | 2.51%                |
|                                     | $n_a = 3$ | 8.90       | 33.70      | $1.56 \times 10^{-8}$ | 1.59%                |
|                                     | $n_a = 4$ | 8.15       | 38.60      | $1.57 \times 10^{-8}$ | 1.50%                |
|                                     | $n_a = 5$ | 7.25       | 41.25      | $1.57 \times 10^{-8}$ | 1.53%                |
|                                     | $n_a = 6$ | 6.60       | 43.60      | $1.56 \times 10^{-8}$ | 1.26%                |
|                                     | $n_a = 7$ | 6.20       | 46.40      | $1.57 \times 10^{-8}$ | 1.64%                |
|                                     | $n_a = 8$ | 6.20       | 51.60      | $1.57 \times 10^{-8}$ | 1.05%                |

#### 345 4.4. Example 4: A spatial truss structure

346 The fourth example is a 120-bar spatial truss structure under vertical loads [19, 20], as depicted in  
347 Fig. 6. The finite element of the structure is built using OpenSees and it contains 49 nodes and 120 truss  
348 members. The cross-sectional area and Young's modulus, denoted  $A$  and  $E$ , are assumed to be the same  
349 for all members. Thirteen vertical loads, denoted  $P_0 - P_{12}$ , are applied to nodes 0 - 12, respectively. The  
350 performance function is formulated as follows:

$$g(\mathbf{X}) = \Delta - V_0(A, E, P_0 - P_{12}), \quad (36)$$

351 where  $V_0$  denotes the vertical displacement of node 0;  $\Delta$  is the associated threshold, which is specified as  
352 100 mm;  $A$ ,  $E$ ,  $P_0 - P_{12}$  are treated as 15 random variables, as listed in Table 7.

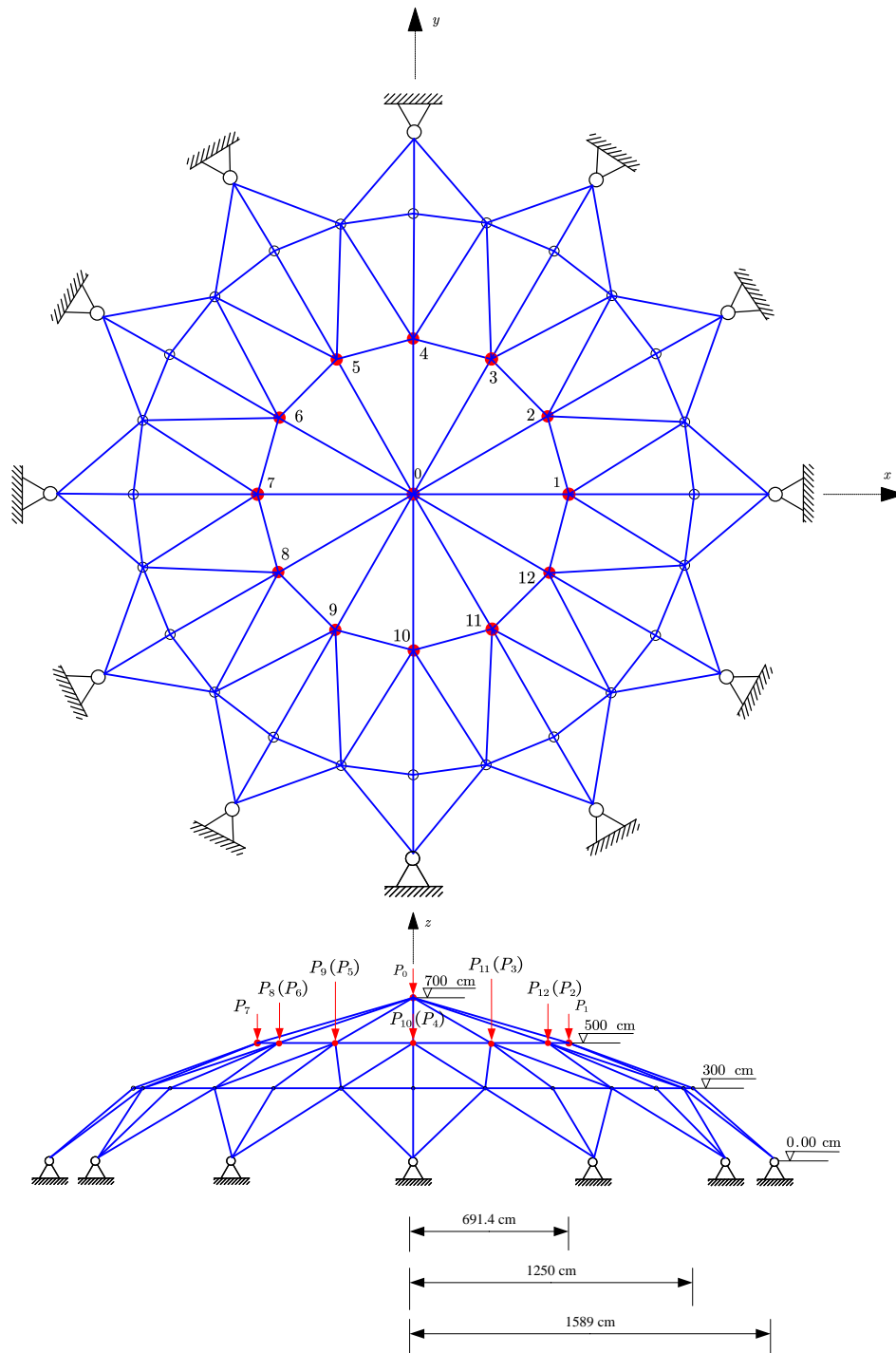


Figure 6: A 120-bar space truss structure subject to thirteen vertical loads.

Table 7: Random variables for Example 4.

| Variable          | Distribution | Mean                  | COV  |
|-------------------|--------------|-----------------------|------|
| $A$               | Normal       | 2,000 mm <sup>2</sup> | 0.10 |
| $E$               | Normal       | 200 GPa               | 0.10 |
| $P_0$             | Lognormal    | 500 kN                | 0.20 |
| $P_1 \sim P_{12}$ | Lognormal    | 60 kN                 | 0.15 |

353 The reliability analysis results of several methods are summarized in Table 8. To provide a reference  
354 solution, the important sampling (IS) method available in UQLab [36] is used instead of MCS. The reference  
355 failure probability obtained is  $1.87 \times 10^{-7}$  with a COV of 1.98%, at the expense of 30,142  $\mathcal{G}$ -function  
356 evaluations. When  $n_a = 1$ , the three PBALC methods, on average, demand slightly fewer  $\mathcal{G}$  function calls  
357 compared to the proposed SBALQ method, but they exhibit higher variability. When  $n_a = 4$ , although  
358 the PABQ method outperforms the proposed SBALQ method in terms of the average number of iterations,  
359 the former yields a rather large COV of 162.04%. The eAK-MCS method fails to produce results due to  
360 computer memory issues. As for the proposed SBALQ method itself, the average number of iterations can  
361 be reduced from 37.05 to 12.55 (although the average total number of performance function calls increases)  
362 when  $n_a$  is increased from 1 to 8. In addition, the proposed method can produce a nearly unbiased failure  
363 probability mean with a COV less than 8% in each case.

#### 364 4.5. Example 5: A jet engine turbine blade

365 The final example concerns a turbine blade from a jet engine (as depicted in Fig. 7), which is available  
366 in the Partial Differential Equation Toolbox of Matlab R2022b. The turbine blade is made of nickel-based  
367 alloy (NIMONIC 90) with Young's modulus  $E$ , Poisson's ratio  $\nu$  and the coefficient of thermal expansion  
368  $CTE$ . The root face (face 3 in Fig. 7(a)) in contact with other metal is fixed. Pressure load  $p_1$  is applied  
369 to the pressure sides, and pressure loads  $p_2$  are applied to the suction sides. The finite-element model  
370 is discretized by linear tetrahedral elements with the maximum element size 0.01 m, which is shown in  
371 Fig. 7(b). One typical cause of the blade failure is mechanical stress, and hence we define the following



Table 8: Reliability analysis results of Example 4 by several methods.

| Method                              |           | $N_{iter}$ | $N_{call}$ | $\hat{P}_f$           | $\delta_{\hat{P}_f}$ |
|-------------------------------------|-----------|------------|------------|-----------------------|----------------------|
| IS                                  |           | -          | 30,142     | $1.87 \times 10^{-7}$ | 1.98%                |
| PBALC1 ( $\epsilon_1 = 5\%$ )       | $n_a = 1$ | 36.25      | 45.25      | $1.85 \times 10^{-7}$ | 7.39%                |
| PBALC2 ( $\epsilon_2 = 5\%$ )       | $n_a = 1$ | 30.45      | 39.45      | $1.84 \times 10^{-7}$ | 6.36%                |
| PBALC3 ( $\epsilon_3 = 10\%$ )      | $n_a = 1$ | 32.75      | 41.75      | $1.84 \times 10^{-7}$ | 7.44%                |
| PABQ                                | $n_a = 4$ | 9.70       | 44.80      | $1.95 \times 10^{-7}$ | 162.04%              |
| eAK-MCS                             | $n_a = 4$ | -          | -          | -                     | -                    |
|                                     | $n_a = 1$ | 37.05      | 46.05      | $1.82 \times 10^{-7}$ | 3.39%                |
|                                     | $n_a = 2$ | 22.70      | 53.40      | $1.80 \times 10^{-7}$ | 6.87%                |
|                                     | $n_a = 3$ | 20.20      | 67.60      | $1.82 \times 10^{-7}$ | 6.48%                |
| Proposed SBALQ ( $\epsilon = 4\%$ ) | $n_a = 4$ | 17.20      | 74.80      | $1.85 \times 10^{-7}$ | 5.09%                |
|                                     | $n_a = 5$ | 14.95      | 79.75      | $1.82 \times 10^{-7}$ | 7.93%                |
|                                     | $n_a = 6$ | 14.30      | 89.80      | $1.81 \times 10^{-7}$ | 6.54%                |
|                                     | $n_a = 7$ | 13.15      | 95.05      | $1.83 \times 10^{-7}$ | 6.64%                |
|                                     | $n_a = 8$ | 12.55      | 102.40     | $1.82 \times 10^{-7}$ | 6.42%                |

372 performance function:

$$g(\mathbf{X}) = \sigma_{th} - \sigma_{max}(E, \nu, CET, p_1, p_2), \quad (37)$$

373 where  $\sigma_{th} = 0.8$  GPa is the threshold for the maximum von Mises stress  $\sigma_{max}$  of the blade;  $E$ ,  $\nu$ ,  $CET$ ,  $p_1$   
374 and  $p_2$  are five random variables, as listed in Table 9.

375 Table 10 reports the reliability analysis results of several methods, i.e., IS [36], PBALC1, PBALC2,  
376 PBALC3, PABQ, eAK-MCS and the proposed SBALQ method. IS [36] was implemented to provide a  
377 reference value for the failure probability. However, its results were not available because something went  
378 wrong during the analysis. As an alternative, the reference failure probability is taken as  $1.25 \times 10^{-8}$  (with a  
379 COV of 0.77%), which is the mean value given by PBALC1 ( $\epsilon_1 = 5\%$ ) with 20 runs. For  $n_a = 1$ , PBALC1,

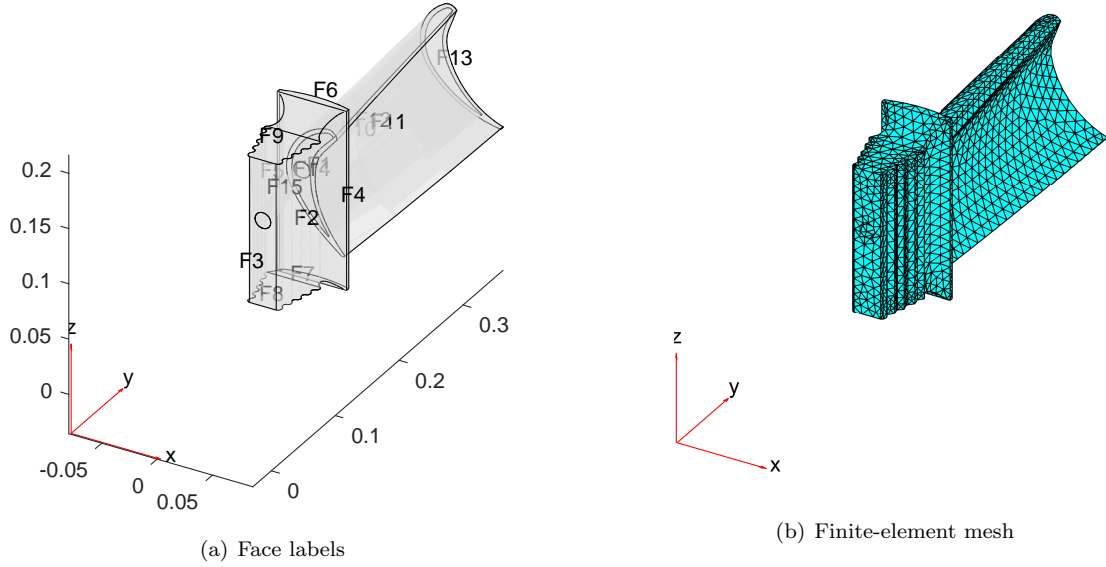


Figure 7: A jet engine turbine blade.

Table 9: Random variables for Example 5.

| Variable | Distribution | Mean                      | COV  |
|----------|--------------|---------------------------|------|
| $E$      | Normal       | 220 GPa                   | 0.10 |
| $\nu$    | Normal       | 0.30                      | 0.05 |
| $CET$    | Uniform      | $1.25 \times 10^{-7}$ 1/K | 0.05 |
| $p_1$    | Gumbel       | 500 kPa                   | 0.15 |
| $p_2$    | Gumbel       | 450 kPa                   | 0.15 |

380 PBALC2 and PBALC3 methods and the proposed SBALQ method can produce quite similar mean values  
 381 for the failure probability with rather small COVs. Among them, the proposed method requires the fewest  
 382  $\mathcal{G}$ -function calls. When  $n_a = 4$ , PABQ gives a biased mean for the failure probability, while processing  
 383 a large COV. Like IS, eAK-MCS encountered an error when running the finite element analysis, so no  
 384 results can be given. On the contrary, the proposed method ( $n_a = 4$ ) performs well, as do other cases (i.e.,  
 385  $n_a = 1, 2, 3, 5, 6, 7, 8$ ). Moreover, the number of iterations required by the proposed method decreases as  $n_a$   
 386 increases from 1 to 5, but increases as  $n_a$  increases from 5 to 8.

Table 10: Reliability analysis results of Example 5 by several methods.

| Method                              |           | $N_{iter}$ | $N_{call}$ | $\hat{P}_f$           | $\delta_{\hat{P}_f}$ |
|-------------------------------------|-----------|------------|------------|-----------------------|----------------------|
| IS                                  |           | -          | -          | -                     | -                    |
| PBALC1 ( $\epsilon_1 = 5\%$ )       | $n_a = 1$ | 28.85      | 37.85      | $1.25 \times 10^{-8}$ | 0.77%                |
| PBALC2 ( $\epsilon_2 = 5\%$ )       | $n_a = 1$ | 41.00      | 50.00      | $1.25 \times 10^{-8}$ | 1.45%                |
| PBALC3 ( $\epsilon_3 = 10\%$ )      | $n_a = 1$ | 38.30      | 47.30      | $1.24 \times 10^{-8}$ | 2.04%                |
| PABQ                                | $n_a = 4$ | 3.95       | 21.80      | $1.01 \times 10^{-8}$ | 34.05%               |
| eAK-MCS                             | $n_a = 4$ | -          | -          | -                     | -                    |
|                                     | $n_a = 1$ | 18.65      | 27.65      | $1.25 \times 10^{-8}$ | 1.63%                |
|                                     | $n_a = 2$ | 12.00      | 32.00      | $1.26 \times 10^{-8}$ | 2.92%                |
|                                     | $n_a = 3$ | 10.50      | 38.50      | $1.25 \times 10^{-8}$ | 1.42%                |
|                                     | $n_a = 4$ | 8.35       | 39.40      | $1.26 \times 10^{-8}$ | 1.10%                |
| Proposed SBALQ ( $\epsilon = 4\%$ ) | $n_a = 5$ | 8.05       | 45.25      | $1.25 \times 10^{-8}$ | 1.02%                |
|                                     | $n_a = 6$ | 8.55       | 55.30      | $1.25 \times 10^{-8}$ | 0.84%                |
|                                     | $n_a = 7$ | 8.15       | 60.05      | $1.25 \times 10^{-8}$ | 0.59%                |
|                                     | $n_a = 8$ | 8.95       | 73.60      | $1.25 \times 10^{-8}$ | 1.28%                |

387 **Remark.** As observed in the five numerical examples above, the average number of iterations required  
388 by the proposed method does not always decrease as  $n_a$  increases. This means that if  $n_a$  cores are used  
389 for an expensive  $\mathcal{G}$  function, a too large  $n_a$  may not lead to a reduction in the overall computation time.  
390 According to our computational experience,  $n_a = 4 - 6$  should be sufficient.

## 391 5. Concluding remarks

392 This study presents an innovative method termed ‘semi-Bayesian active learning quadrature’ (SBALQ)  
393 for structural reliability analysis, particularly for evaluating extremely small failure probabilities. The main  
394 contributions lie in the development of two key components for active learning (i.e., stopping criterion and

395 learning function) based on the well-established Bayesian failure probability inference framework, while  
396 avoiding the use of the posterior variance of the failure probability, which is expensive to evaluate. First, we  
397 introduce a new stopping criterion by exploring the structure of the posterior mean of the failure probability  
398 only. This criterion involves two analytically intractable integrals. Second, a numerical integration technique  
399 called ‘hyper-shell simulation’ is devised to approximate the integrals. Third, we propose a new learning  
400 function based on the proposed stopping criterion, and by maximizing it a single point can be identified  
401 at each iteration of the active learning phase. Fourth, the proposed learning function is further modified  
402 by multiplying an influence function so as to enable multi-point selection and hence parallel distributed  
403 processing. It is empirically shown from five numerical examples that the proposed SBALQ method is  
404 capable of estimating very low failure probabilities in the order of  $10^{-7}$  -  $10^{-9}$ , while maintaining desired  
405 efficiency and accuracy. It is worth noting that the computational efficiency can be further improved by  
406 leveraging the parallelizability inherent in the proposed approach.

407 The proposed method, in its current form, performs poorly in high dimensions due to the limitations  
408 of GP and HSS. Consequently, a promising avenue for future research lies in the integration of effective  
409 dimension reduction techniques. Furthermore, it is still challenging to apply the proposed method to highly  
410 nonlinear problems when using the squared exponential kernel, as it implies a smooth assumption.

#### 411 **Declaration of competing interest**

412 The authors declare that they have no known competing financial interests or personal relationships that  
413 could have appeared to influence the work reported in this paper.

#### 414 **Acknowledgments**

415 Chao Dang is mainly supported by China Scholarship Council (CSC). Michael Beer would like to thank  
416 the support of the National Natural Science Foundation of China under grant number 72271025.

## 417 Data availability

418 Data will be made available on request.

## 419 Appendix A. Generation of uniform random samples in the $h - 1$ inner hyper-shells

420 The procedure for generating  $N_i$  uniform random samples in the  $h - 1$  inner hyper-shells is as follows:

- 421 1. Draw  $N_i$  random samples that are uniformly distributed on  $[R_{i-1}^d, R_i^d]$ , denoted as  $\{v^{(j)} : j = 1, 2, \dots, N_i\}$ ;
- 422 2. Generate  $N_i$  random samples from  $\phi_{\mathcal{U}}(\mathbf{u})$ , denoted as  $\{\mathbf{u}^{(j)} : j = 1, 2, \dots, N_i\}$ ;
- 423 3. Obtain the  $j$ -th sample in the  $i$ -th inner hyper-shell by  $\mathbf{u}^{(i,j)} = \frac{\sqrt[3]{v^{(j)}}\mathbf{u}^{(j)}}{\|\mathbf{u}^{(j)}\|}$ .

## 424 Appendix B. Generation of random samples in the outermost hyper-shell

425 The procedure for generating  $N_i$  random samples from  $\psi^{(h)}(\mathbf{u})$  in the outermost hyper-shell is as follows:

- 426 1. Draw  $N_i$  random samples that are uniformly distributed on  $[1 - 10^{-(h-1)}, 1]$ , which are denoted as  
427  $\{p^j : j = 1, 2, \dots, N_i\}$ ;
- 428 2. Generate  $N_i$  random samples from  $\phi_{\mathcal{U}}(\mathbf{u})$ , denoted as  $\{\mathbf{u}^{(j)} : j = 1, 2, \dots, N_i\}$ ;
- 429 3. Obtain the  $j$ -th sample in the outermost hyper-shell by  $\mathbf{u}^{(i,j)} = \frac{\sqrt{\chi_d^{-2}(p^j)}\mathbf{u}^{(j)}}{\|\mathbf{u}^{(j)}\|}$ .

## 430 References

- 431 [1] G. Rubino, B. Tuffin, et al., Rare event simulation using Monte Carlo methods, Vol. 73, Wiley Online Library, 2009.
- 432 [2] S.-K. Au, J. L. Beck, A new adaptive importance sampling scheme for reliability calculations, Structural Safety 21 (2)  
433 (1999) 135–158. doi:[https://doi.org/10.1016/S0167-4730\(99\)00014-4](https://doi.org/10.1016/S0167-4730(99)00014-4).
- 434 [3] I. Papaioannou, S. Geyer, D. Straub, Improved cross entropy-based importance sampling with a flexible mixture model,  
435 Reliability Engineering & System Safety 191 (2019) 106564. doi:<https://doi.org/10.1016/j.ress.2019.106564>.
- 436 [4] J. Xian, Z. Wang, Relaxation-based importance sampling for structural reliability analysis, Structural Safety 106 (2024)  
437 102393. doi:<https://doi.org/10.1016/j.strusafe.2023.102393>.
- 438 [5] S.-K. Au, J. L. Beck, Estimation of small failure probabilities in high dimensions by subset simulation, Probabilistic  
439 Engineering Mechanics 16 (4) (2001) 263–277. doi:[https://doi.org/10.1016/S0266-8920\(01\)00019-4](https://doi.org/10.1016/S0266-8920(01)00019-4).
- 440 [6] J. Nie, B. R. Ellingwood, Directional methods for structural reliability analysis, Structural Safety 22 (3) (2000) 233–249.  
441 doi:[https://doi.org/10.1016/S0167-4730\(00\)00014-X](https://doi.org/10.1016/S0167-4730(00)00014-X).

- 442 [7] P.-S. Koutsourelakis, H. J. Pradlwarter, G. I. Schuëller, Reliability of structures in high dimensions, part I: algorithms and  
443 applications, *Probabilistic Engineering Mechanics* 19 (4) (2004) 409–417. doi:[https://doi.org/10.1016/j.probengmech.  
444 2004.05.001](https://doi.org/10.1016/j.probengmech.2004.05.001).
- 445 [8] A. M. Hasofer, N. C. Lind, Exact and invariant second-moment code format, *Journal of the Engineering Mechanics Division*  
446 100 (1) (1974) 111–121. doi:<https://doi.org/10.1061/JMCEA3.0001848>.
- 447 [9] K. W. Breitung, *Asymptotic approximations for probability integrals*, Springer, 2006.
- 448 [10] L. Tvedt, Distribution of quadratic forms in normal space—application to structural reliability, *Journal of Engineering*  
449 *Mechanics* 116 (6) (1990) 1183–1197. doi:[https://doi.org/10.1061/\(ASCE\)0733-9399\(1990\)116:6\(1183\)](https://doi.org/10.1061/(ASCE)0733-9399(1990)116:6(1183)).
- 450 [11] G. Blatman, B. Sudret, An adaptive algorithm to build up sparse polynomial chaos expansions for stochastic finite element  
451 analysis, *Probabilistic Engineering Mechanics* 25 (2) (2010) 183–197. doi:[https://doi.org/10.1016/j.probengmech.  
452 2009.10.003](https://doi.org/10.1016/j.probengmech.2009.10.003).
- 453 [12] I. Kaymaz, Application of kriging method to structural reliability problems, *Structural Safety* 27 (2) (2005) 133–151.  
454 doi:<https://doi.org/10.1016/j.strusafe.2004.09.001>.
- 455 [13] C. Song, R. Kawai, Monte Carlo and variance reduction methods for structural reliability analysis: A comprehensive  
456 review, *Probabilistic Engineering Mechanics* (2023) 103479doi:<https://doi.org/10.1016/j.probengmech.2023.103479>.
- 457 [14] B. J. Bichon, M. S. Eldred, L. P. Swiler, S. Mahadevan, J. M. McFarland, Efficient global reliability analysis for nonlinear  
458 implicit performance functions, *AIAA Journal* 46 (10) (2008) 2459–2468. doi:<https://doi.org/10.2514/1.34321>.
- 459 [15] B. Echard, N. Gayton, M. Lemaire, AK-MCS: an active learning reliability method combining Kriging and Monte Carlo  
460 simulation, *Structural Safety* 33 (2) (2011) 145–154. doi:<https://doi.org/10.1016/j.strusafe.2011.01.002>.
- 461 [16] R. Teixeira, M. Nogal, A. O’Connor, Adaptive approaches in metamodel-based reliability analysis: A review, *Structural*  
462 *Safety* 89 (2021) 102019. doi:<https://doi.org/10.1016/j.strusafe.2020.102019>.
- 463 [17] S. S. Afshari, F. Enayatollahi, X. Xu, X. Liang, Machine learning-based methods in structural reliability analysis: A  
464 review, *Reliability Engineering & System Safety* 219 (2022) 108223. doi:<https://doi.org/10.1016/j.res.2021.108223>.
- 465 [18] M. Moustapha, S. Marelli, B. Sudret, Active learning for structural reliability: Survey, general framework and benchmark,  
466 *Structural Safety* 96 (2022) 102174. doi:<https://doi.org/10.1016/j.strusafe.2021.102174>.
- 467 [19] C. Dang, P. Wei, J. Song, M. Beer, Estimation of failure probability function under imprecise probabilities by active  
468 learning–augmented probabilistic integration, *ASCE-ASME Journal of Risk and Uncertainty in Engineering Systems,*  
469 *Part A: Civil Engineering* 7 (4) (2021) 04021054. doi:<https://doi.org/10.1061/AJRUA6.0001179>.
- 470 [20] C. Dang, P. Wei, M. G. Faes, M. A. Valdebenito, M. Beer, Parallel adaptive Bayesian quadrature for rare event estimation,  
471 *Reliability Engineering & System Safety* 225 (2022) 108621. doi:<https://doi.org/10.1016/j.res.2022.108621>.
- 472 [21] C. Dang, M. A. Valdebenito, M. G. Faes, P. Wei, M. Beer, Structural reliability analysis: A Bayesian perspective,  
473 *Structural Safety* 99 (2022) 102259. doi:<https://doi.org/10.1016/j.strusafe.2022.102259>.
- 474 [22] C. Dang, M. A. Valdebenito, J. Song, P. Wei, M. Beer, Estimation of small failure probabilities by partially Bayesian

- 475 active learning line sampling: Theory and algorithm, *Computer Methods in Applied Mechanics and Engineering* 412  
476 (2023) 116068. doi:<https://doi.org/10.1016/j.cma.2023.116068>.
- 477 [23] C. Dang, M. A. Valdebenito, M. G. Faes, J. Song, P. Wei, M. Beer, Structural reliability analysis by line sampling: A  
478 Bayesian active learning treatment, *Structural Safety* 104 (2023) 102351. doi:[https://doi.org/10.1016/j.strusafe.  
479 2023.102351](https://doi.org/10.1016/j.strusafe.2023.102351).
- 480 [24] C. Dang, M. Beer, Bayesian active learning line sampling with log-normal process for rare-event probability estimation,  
481 *Reliability Engineering & System Safety* (2024) In Press.
- 482 [25] Z. Hu, C. Dang, L. Wang, M. Beer, Parallel Bayesian probabilistic integration for structural reliability analysis with small  
483 failure probabilities, *Structural Safety* 106 (2024) 102409. doi:<https://doi.org/10.1016/j.strusafe.2023.102409>.
- 484 [26] C. Dang, M. G. Faes, M. A. Valdebenito, P. Wei, M. Beer, Partially Bayesian active learning cubature for structural  
485 reliability analysis with extremely small failure probabilities, *Computer Methods in Applied Mechanics and Engineering*  
486 422 (2024) 116828. doi:<https://doi.org/10.1016/j.cma.2024.116828>.
- 487 [27] Z. Chen, G. Li, J. He, Z. Yang, J. Wang, A new parallel adaptive structural reliability analysis method based on importance  
488 sampling and K-medoids clustering, *Reliability Engineering & System Safety* 218 (2022) 108124. doi:[https://doi.org/  
489 10.1016/j.ress.2021.108124](https://doi.org/10.1016/j.ress.2021.108124).
- 490 [28] G. Li, T. Wang, Z. Chen, J. He, X. Wang, X. Du, RBIK-SS: A parallel adaptive structural reliability analysis method for  
491 rare failure events, *Reliability Engineering & System Safety* 239 (2023) 109513. doi:[https://doi.org/10.1016/j.ress.  
492 2023.109513](https://doi.org/10.1016/j.ress.2023.109513).
- 493 [29] M. Su, G. Xue, D. Wang, Y. Zhang, Y. Zhu, A novel active learning reliability method combining adaptive Kriging and  
494 spherical decomposition-MCS (AK-SDMCS) for small failure probabilities, *Structural and Multidisciplinary Optimization*  
495 62 (2020) 3165–3187. doi:<https://doi.org/10.1007/s00158-020-02661-w>.
- 496 [30] A. Persoons, P. Wei, M. Broggi, M. Beer, A new reliability method combining adaptive Kriging and active variance  
497 reduction using multiple importance sampling, *Structural and Multidisciplinary Optimization* 66 (6) (2023) 144. doi:  
498 <https://doi.org/10.1007/s00158-023-03598-6>.
- 499 [31] D. Zhan, J. Qian, Y. Cheng, Pseudo expected improvement criterion for parallel EGO algorithm, *Journal of Global*  
500 *Optimization* 68 (2017) 641–662. doi:<https://doi.org/10.1007/s10898-016-0484-7>.
- 501 [32] N. Razaaly, P. M. Congedo, Extension of AK-MCS for the efficient computation of very small failure probabilities,  
502 *Reliability Engineering & System Safety* 203 (2020) 107084. doi:<https://doi.org/10.1016/j.ress.2020.107084>.
- 503 [33] J. Bect, L. Li, E. Vazquez, Bayesian subset simulation, *SIAM/ASA Journal on Uncertainty Quantification* 5 (1) (2017)  
504 762–786. doi:<https://doi.org/10.1137/16M1078276>.
- 505 [34] C. G. Bucher, U. Bourgund, A fast and efficient response surface approach for structural reliability problems, *Structural*  
506 *Safety* 7 (1) (1990) 57–66. doi:[https://doi.org/10.1016/0167-4730\(90\)90012-E](https://doi.org/10.1016/0167-4730(90)90012-E).
- 507 [35] J. Zhou, A. S. Nowak, Integration formulas to evaluate functions of random variables, *Structural Safety* 5 (4) (1988)

508 267–284. doi:[https://doi.org/10.1016/0167-4730\(88\)90028-8](https://doi.org/10.1016/0167-4730(88)90028-8).

509 [36] S. Marelli, R. Schöbi, B. Sudret, UQLab user manual – Structural reliability (Rare event estimation), Tech. rep., Chair of  
510 Risk, Safety and Uncertainty Quantification, ETH Zurich, Switzerland, report UQLab-V2.0-107 (2022).